

Time-consistent mean-variance portfolio optimization: a numerical impulse control approach

Pieter Van Staden* Duy-Minh Dang[†] Peter A. Forsyth[‡]

Abstract

We investigate the time-consistent mean-variance (MV) portfolio optimization problem, popular in investment-reinsurance and investment-only applications, under a realistic context that involves the simultaneous application of different types of investment constraints and modelling assumptions, for which a closed-form solution is not known to exist. We develop an efficient numerical partial differential equation method for determining the optimal control for this problem. Central to our method is a combination of (i) an impulse control formulation of the MV investment problem, and (ii) a discretized version of the dynamic programming principle enforcing a time-consistency constraint. We impose realistic investment constraints, such as no trading if insolvent, leverage restrictions and different interest rates for borrowing/lending. Our method requires solution of linear partial integro-differential equations between intervention times, which is numerically simple and computationally effective. The proposed method can handle both continuous and discrete rebalancings. We study the substantial effect and economic implications of realistic investment constraints and modelling assumptions on the MV efficient frontier and the resulting investment strategies. This includes (i) a comprehensive comparison study of the pre-commitment and time-consistent optimal strategies, and (ii) an investigation on the significant impact of a wealth-dependent risk aversion parameter on the optimal controls.

Keywords: Asset allocation, constrained optimal control, time-consistent, pre-commitment, impulse control

JEL Subject Classification: G11, C61

1 Introduction

Originating with Markowitz (1952), the standard criterion in modern portfolio theory has been maximizing the (terminal) expected return of a portfolio, given an acceptable level of risk, where risk is quantified by the (terminal) variance of the portfolio returns. This is referred to as mean-variance (MV) portfolio optimization. Mean-variance strategies are appealing due to their intuitive nature, since the results can be easily interpreted in terms of the trade-off between risk (variance) and reward (expected return).

Broadly speaking, there are three main approaches, or strategies, to perform MV optimization, namely (i) the pre-commitment approach, (ii) the dynamically optimal approach, and (iii) the time-consistent (or game theoretical) approach. The pre-commitment approach (see, for example, Dang and Forsyth (2014); Li and Ng (2000); Zhou and Li (2000)) is time-inconsistent in the sense that, for

*School of Mathematics and Physics, The University of Queensland, St Lucia, Brisbane 4072, Australia, email: pieter.vanstaden@uq.edu.au

[†]School of Mathematics and Physics, The University of Queensland, St Lucia, Brisbane 4072, Australia, email: duyminh.dang@uq.edu.au

[‡]Cheriton School of Computer Science, University of Waterloo, Waterloo ON, Canada, N2L 3G1, paforsyt@uwaterloo.ca

35 $\Delta t > 0$, the MV optimal strategy for time $t + 2\Delta t$, computed at time t , may not agree with the MV
36 optimal strategy for time $t + 2\Delta t$, computed at time $t + \Delta t$. This time-inconsistency is addressed in the
37 dynamically optimal approach of Pedersen and Peskir (2017) by recomputing the pre-commitment MV
38 optimal strategy at each time instant, thereby achieving instantaneous optimality by performing an
39 infinite number of optimization problems. The time-consistent approach (Basak and Chabakauri, 2010;
40 Bjork and Murgoci, 2010; Cong and Oosterlee, 2016; Wang and Forsyth, 2011) addresses the time-
41 inconsistency by imposing a time-consistency constraint, i.e. constraining the original MV optimization
42 problem to ensure that the optimal strategy for time $t + 2\Delta t$, computed at time t , necessarily agrees
43 with the optimal strategy for time $t + 2\Delta t$, computed at time $t + \Delta t$.

44 The pre-commitment MV perspective typically requires that an investor/insurer make a credible
45 commitment that the MV-optimal strategy, computed at time zero, will be followed over the entire
46 investment time horizon, which could be substantially long (e.g. pension fund investments). This may
47 not be feasible in institutional settings. The time-consistent MV approach has received considerable
48 attention in recent literature; see, for example, Alia et al. (2016); Bensoussan et al. (2014); Cui
49 et al. (2015); Li et al. (2015c); Liang and Song (2015); Sun et al. (2016); Zhang and Liang (2017),
50 among many other publications. In particular, as evidenced by these publications, this approach has
51 been very popular in institutional settings - especially in insurance-related applications, where MV-
52 utility insurers are typically concerned with investment-reinsurance or investment-only optimization
53 problems.

54 With the notable exception of Wang and Forsyth (2011) and Cong and Oosterlee (2016), virtually
55 all of the available literature on time-consistent MV optimization is based on solving the resulting equa-
56 tions using closed-form (analytical) techniques, which necessarily requires very restrictive, and hence
57 unrealistic, modelling and investment assumptions. These assumptions include continuous rebalanc-
58 ing, zero transaction costs, allowing insolvency and infinite leverage. Formulating problems without
59 realistic investment constraints usually results in conclusions that are difficult to justify, and/or are
60 potentially infeasible to implement in practice.

61 Specifically, in the time-consistent MV literature, the effect of the commonly encountered assump-
62 tion, namely trading continues even if the investor is insolvent, is rarely considered. A few exceptions
63 include Zhou et al. (2016), where the bankruptcy implications from multi-period time-consistent MV
64 and pre-commitment MV optimization problems are compared; however, a bankruptcy constraint is
65 not explicitly enforced in this work. A conclusion in Zhou et al. (2016) is that the time-consistent
66 strategy “can diversify bankruptcy risk efficiently”, since the resulting probability of insolvency over
67 the investment time horizon is lower, and therefore, the time-consistent strategy might be preferred
68 by a rational investor over the pre-commitment strategy. However, in practice, real portfolios have
69 bankruptcy constraints. Hence, such conclusions are questionable. In the case of other time-consistent
70 MV applications, such as asset-liability management, the explicit incorporation of insolvency consid-
71 erations is critical to ensure that the results are of any practical use. The analytical solutions in,
72 for example, Wei et al. (2013) and Wei and Wang (2017), while useful, necessarily assume trading
73 continues in the case of insolvency.

74 Moreover, in the time-consistent MV literature, it is typical for analytical techniques to allow for a
75 leverage ratio, i.e. the ratio of the investment in the risky asset to the total wealth, substantially larger
76 than a ratio that brokers would typically allow retail investors or financial regulators would likely allow
77 institutions to undertake in practice. More specifically, while a leverage ratio of around 1.5 times is
78 typically allowed in practice (for retail investors), some of the analytical techniques illustrated in the
79 available literature call for much larger leverage ratios, for example 2.4 times in Li et al. (2012), 3 times
80 in Zeng et al. (2013), 2.6 times in Liang and Song (2015), 2.5 times in Li et al. (2015c), and as high as
81 14 times in Li et al. (2015a), none of which are practically feasible, and which only further increases
82 the probability of insolvency. In a number of publications, a leverage constraint is completely ignored,

83 such as Lioui (2013), and this potentially leads to misplaced economic conclusions. For example, it
84 is concluded in Lioui (2013) that the time-consistent strategy is preferred over the pre-commitment
85 strategy, since the latter requires “huge and unrealistic positions in risky assets; in some cases, the pre-
86 commitment strategy is more than 60 times the time consistent strategy”. However, such a conclusion
87 appears unconvincing, since the pre-commitment MV strategy’s positions in the risky asset would have
88 been significantly smaller, if a realistic leverage constraint had been incorporated into the problem
89 formulation.

90 In addition, failing to incorporate transaction costs may also lead to strategies which are not
91 economically viable. For example, a numerical example provided in Li et al. (2015b), where no
92 transaction costs are considered, shows the risky asset price undergoing reasonable changes over the
93 course of a month, but the resulting time-consistent MV-optimal analytical solution calls for an almost
94 three-fold increase in the risky asset holdings as the risky asset price declines, only to unwind the entire
95 position again as the risky asset price recovers at the end of the month.

96 Also, any strategy which allows leverage, even if limited, should take into account that borrowing
97 rates will be larger than lending rates, which will clearly affect any conclusions drawn regarding trading
98 strategies.

99 Furthermore, the use of a wealth-dependent risk-aversion parameter has been popular in time-
100 consistent MV literature, especially in insurance-related applications, such as Zeng and Li (2011), Wei
101 et al. (2013), Li and Li (2013), as well as Liang and Song (2015)). While arguments in favour of,
102 for example, a risk aversion parameter inversely proportional to wealth appear to be reasonable when
103 considered in the absence of investment constraints (see for example Bjork et al. (2014) and Li and
104 Li (2013)), in the presence of realistic constraints this formulation may have some unintended and
105 undesirable economic consequences from both a risk and a return perspective, as will become evident
106 below.

107 As a result, in order to ensure that economically viable strategies can be developed and econom-
108 ically reasonable conclusions can be drawn, a number of realistic investment constraints need to be
109 incorporated simultaneously as part of the formulation of the MV optimization problem. Such a
110 comprehensive treatment with realistic investment constraints cannot be expected to yield analytical
111 solutions, and hence a fully numerical solution approach must be used in this case. This is the main
112 focus of this work.

113 The literature on numerical methods for time-consistent MV portfolio optimization is virtually
114 limited to the case of diffusion dynamics, i.e. Geometric Brownian Motion, for the risky asset, including
115 notable works of Cong and Oosterlee (2016); Wang and Forsyth (2011). However, it is well-documented
116 in the finance literature that jumps are often present in the price processes of risky assets (see, for
117 example, Cont and Tankov (2004); Ramezani and Zeng (2007)). Jump processes permit modelling
118 of non-normal asset returns and fat tails. We focus on jump-diffusions in this work, since previous
119 studies indicate that mean-reverting stochastic volatility processes have a very small effect on the
120 efficient frontier for long term (> 10 years) investors (Ma and Forsyth, 2016). Using a Monte Carlo
121 approach, Cong and Oosterlee (2016) compare pre-commitment and time-consistent policies with
122 leverage and bankruptcy constraints in the case of diffusion dynamics.¹ In the present work, we
123 go a step forward by considering both the continuous and discrete rebalancing versions of the time-
124 consistent MV portfolio optimization problem with jump-diffusion dynamics for the risky asset and
125 realistic investment constraints, such as transaction costs and different borrowing and lending interest
126 rates. Moreover, we also provide a comprehensive comparison between the time-consistency and pre-
127 commitment approaches, not only in terms of the resulting efficient frontiers, but also in terms of the
128 optimal investment policies over time under the above-mentioned realistic context. Furthermore, our
129 use of partial integro-differential equation (PIDE) methods for solution of the optimal control problem

¹The bankruptcy constraint in (Cong and Oosterlee, 2016) is not quite the same as considered in this work.

130 allows us to illustrate the strategies in terms of easy-to-interpret heat maps.

131 Generally speaking, the impulse control approach is suitable for many complex situations in
132 stochastic optimal control (Oksendal and Sulem, 2005). In particular, in the context of pre-commitment
133 MV portfolio optimization under jump diffusion, it has been demonstrated in Dang and Forsyth (2014)
134 that an impulse control formulation of the investment problem is very computationally advantageous.
135 This is because an impulse control formulation can avoid the presence of the control in the integrand
136 of the jump terms, which, in turn, facilitates the use of a fast computational method, such as the FFT,
137 for the evaluation of the integral. In addition, an impulse control formulation also allows for efficient
138 handling of realistic modelling assumptions, such as transaction costs.

139 For time-consistent MV portfolio optimization with jump-diffusion dynamics, an impulse control
140 approach can also be utilized to potentially achieve similar computational advantages. In the realistic
141 context considered in this work, applying the popular method of Bjork et al. (2016); Bjork and Murgoci
142 (2014), together with relevant results from Oksendal and Sulem (2005), the value function under an
143 impulse control formulation can be shown to satisfy a strongly coupled, nonlinear system of equations,
144 the so-called an extended Hamilton-Jacobi-Bellman (HJB) quasi-integro-variational inequality. This
145 system of equations must be solved numerically, since a closed-form solution for it is not known to
146 exist, except in special cases. However, it is not clear how such a very complex system of equations can
147 be solved effectively numerically. As a result, in this case, the method of Bjork et al. (2016); Bjork and
148 Murgoci (2014) does not appear to result in equations amenable for computational purposes. Hence,
149 for numerical purposes, an alternative formulation of this problem is desirable.

150 The objective of this paper is two-fold. Firstly, we develop a numerically a computationally effi-
151 cient partial differential equation (PDE) method for the solution of the time-consistent MV portfolio
152 optimization problem under different types of investment constraints and realistic modelling assump-
153 tions. We formulate this problem in such a way as to avoid some of the numerical difficulties resulting
154 from the approach of Bjork et al. (2016); Bjork and Murgoci (2014). Secondly, using actual long-term
155 data, we present a comprehensive study of the impact of simultaneously imposing those investment
156 constraints on the efficient frontier, as well as on the optimal investment strategies, for both the
157 time-consistent and pre-commitment approaches.

158 The main contributions of this paper are as follows.

- 159 • We formulate the time-consistent MV portfolio optimization problem as a system of two-dimensional
160 impulse control problems, with a time-consistency constraint enforced via a discretized version
161 of the dynamic programming principle.

162 This approach results in only linear partial integro-differential equations (PIDEs) to solve be-
163 tween intervention times, which is not only numerically simpler than the approach of Bjork et al.
164 (2016); Bjork and Murgoci (2014), but also computationally efficient.

- 165 • We study the simultaneous application of realistic investment constraints, including (i) discrete
166 (infrequent) rebalancing of the portfolio, (ii) liquidation in the event of insolvency, (iii) leverage
167 constraints, (iv) different interest rates for borrowing and lending, and (v) transaction costs.

- 168 • Since the viscosity solution theory (Crandall et al. (1992)) does not apply in this case, we have
169 no formal proof of convergence of our numerical PDE method. However, we (i) show that our
170 method converges to analytical solutions, where available, and (ii) validate the results from our
171 method using Monte Carlo simulations, where analytical solutions are unavailable.

- 172 • Extensive numerical experiments are conducted with model parameters calibrated to real (i.e.
173 inflation adjusted) long-term US market data (89 years), enabling realistic conclusions to be
174 drawn from the results. Through these experiments, the (significant) impact of various modelling
175 assumptions and investment constraints on the MV efficient frontiers are investigated.

We also present a comprehensive comparison study of the time-consistent and pre-commitment MV optimal strategies.

- For the popular case of a wealth-dependent risk aversion parameter in the time-consistent MV literature, our results show that a seemingly reasonable definition of a wealth-dependent risk-aversion parameter, when used in combination with investment and bankruptcy constraints, can result in conclusions that are not economically reasonable. Not only does this finding pose questions about the use of such wealth-dependent risk aversion parameters in existing time-consistent MV literature, but it also highlights the importance of incorporating realistic constraints in investment models.

The remainder of the paper is organized as follows. Section 2 describes the underlying processes and the impulse control approach, and introduce the pre-commitment and time-consistent MV optimization approaches. A numerical algorithm for solving the time-consistency MV portfolio optimization problem is discussed in detail in Section 3. In Section 4, we discuss the localization and numerical techniques, including discrete rebalancing case. Numerical results are presented and discussed in Section 5. Section 6 concludes the paper and outlines possible future work.

2 Formulation

2.1 Underlying processes

We consider the investment-only problem² from the perspective of a mean-variance investor/insurer investing in portfolios consisting of just two assets, namely a risky asset and a risk-free asset. The lack of allowance for investment in multiple risky assets may initially appear to be overly restrictive, but we argue that this is not the case, due to the following reasons. Firstly, in the applying the approach presented in this paper, we use a diversified index, rather than a single stock (see Section 5). Secondly, in the available analytical solutions for multi-asset time-consistent MV problems, the composition of the risky asset basket remains relatively stable over time (see for example Zeng and Li (2011)). Finally, investment problems with long time horizons has a strong strategic component - the investor/insurer may be more interested in overall global portfolio shifts from stocks to bonds and vice versa³, rather than the more secondary questions relating to risky asset basket compositions.

Let $S(t)$ and $B(t)$ respectively denote the amounts (i.e. total dollars) invested in the risky and risk-free asset, at time $t \in [0, T]$, where $T > 0$ is the fixed horizon investment. Define $t^- = \lim_{\epsilon \downarrow 0} (t - \epsilon)$, $t^+ = \lim_{\epsilon \downarrow 0} (t + \epsilon)$, i.e. t^- (resp. t^+) as the instant of time before (resp. after) the (forward) time t . First, consider the risky asset. Let ξ be a random number representing a jump multiplier, with probability density function (pdf) $p(\xi)$. When a jump occurs, $S(t) = \xi S(t^-)$. As a specific example, we consider two jump distributions for ξ , namely the log-normal distribution (Merton, 1976) and the log-double-exponential distribution (Kou, 2002). Specifically, in the former case, $\log \xi$ is normally distributed, so that

$$p(\xi) = \frac{1}{\xi \sqrt{2\pi\tilde{\gamma}^2}} \exp \left\{ -\frac{(\log \xi - \tilde{m})^2}{2\tilde{\gamma}^2} \right\}, \quad (2.1)$$

²As noted in the conclusion to this paper, we leave the investment-reinsurance problem for future work.

³It is natural for institutions, answerable to their stockholders regarding their chosen investment strategies, to be sensitive to these global trends. As a typical example of an article discussing these trends, see “Global stock optimism drives rotation from bonds into equities”, by Kate Allen, which appeared in the Financial Times (FT) on January 16, 2018.

with mean \tilde{m} and standard deviation $\tilde{\gamma}$, and $E[\xi] = \exp(\tilde{m} + \tilde{\gamma}^2/2)$, where $E[\cdot]$ denotes the expectation operator. In the latter case, $\log \xi$ has an asymmetric double-exponential distribution, so that

$$p(\xi) = \nu \zeta_1 \xi^{-(\zeta_1+1)} \mathbb{I}_{[\xi \geq 1]} + (1 - \nu) \zeta_2 \xi^{\zeta_2-1} \mathbb{I}_{[0 \leq \xi < 1]}. \quad (2.2)$$

Here, $\nu \in [0, 1]$, $\zeta_1 > 1$ and $\zeta_2 > 0$, and $\mathbb{I}_{[A]}$ denotes the indicator function of the event A . Given that a jump occurs, ν is the probability of an upward jump, and $(1 - \nu)$ is the probability of a downward jump. Furthermore, in this case, we have $E[\xi] = \frac{\nu \zeta_1}{\zeta_1 - 1} + \frac{(1 - \nu) \zeta_2}{\zeta_2 + 1}$.

In the context of pre-commitment MV analysis, the results in (Ma and Forsyth, 2016) indicate that the effects of mean-reverting stochastic volatility are unimportant for long-term (i.e. greater than 10 years) investors. Hence we focus here on the effect of jump processes, as a major source of risk. In the absence of control, i.e. if we do not adjust the amount invested according to our control strategy, the amount S invested in the risky asset is assumed to follow the process

$$\frac{dS(t)}{S(t^-)} = (\mu - \lambda \kappa) dt + \sigma dZ + d \left(\sum_{i=1}^{\pi(t)} (\xi_i - 1) \right). \quad (2.3)$$

Here, $\kappa = \mathbb{E}[\xi - 1]$; Z denotes a standard Brownian motion; μ and σ are the real world drift and volatility, respectively; $\pi(t)$ a Poisson process with intensity $\lambda \geq 0$; and ξ_i are i.i.d. random variables having the same distribution as ξ . Moreover, ξ_i , π_t and Z are assumed to all be mutually independent. For later use in the paper, we also define $\kappa_2 = \mathbb{E}[(\xi - 1)^2]$.

It is assumed that the investor can earn a (continuously compounded) rate r_ℓ on cash deposits, and borrow at a rate of $r_b > 0$, with $r_\ell < r_b$. In the absence of control, the dynamics of the amount $B(t)$ invested in the risk-free asset are given by

$$dB(t) = \mathcal{R}(B(t)) B(t) dt, \quad \text{where } \mathcal{R}(B(t)) = r_\ell + (r_b - r_\ell) \mathbb{I}_{[B(t) < 0]}. \quad (2.4)$$

We make the standard assumption that the real world drift rate μ of S is strictly greater than r_ℓ . Since there is only one risky asset, it is never optimal in an MV setting to short stock, i.e. $S(t) \geq 0$, $t \in [0, T]$. However, we do allow short positions in the risk-free asset, i.e. it is possible that $B(t) < 0$, $t \in [0, T]$.

In some of the examples considered in this paper, we assume that, in the absence of the control, the dynamics for $S(t)$ follows GBM. This is implemented by suppressing any possible jumps in (2.3), i.e. by setting the intensity parameter λ to zero.

2.2 Dynamics of the controlled system

We denote by $X(t) = (S(t), B(t))$, $t \in [0, T]$, the multi-dimensional controlled underlying process, and by $x = (s, b)$ the state of the system. Furthermore, the liquidation value of the (controlled) wealth, denoted by $W(t)$. We note that $W(t)$ may include liquidation costs (see (2.8)).

Let $(\mathcal{F}_t)_{t \geq 0}$ be the natural filtration associated with the wealth process $\{W(t) : t \in [0, T]\}$. We use $C_t(\cdot)$ to denote the control, representing a strategy as a function of the underlying state, computed at time $t \in [0, T]$, i.e. $C_t(\cdot) : (X(t), t) \mapsto C_t = C(X(t), t)$, for the time interval $[t, T]$. Following Dang and Forsyth (2014), we make use of impulse controls, which allows for efficient handling of jumps, as well as other realistic modelling assumptions, such as transaction costs. A generic impulse control \mathcal{C}_t is defined as a double, possibly finite, sequence (Oksendal and Sulem, 2005)

$$\mathcal{C}_t = \{t_1, t_2, \dots, t_n; \eta_1, \eta_2, \dots, \eta_n, \dots\}_{n \leq n_{\max}} = \{\{t_n, \eta_n\}\}_{n \leq n_{\max}}, \quad n_{\max} \leq \infty. \quad (2.5)$$

Here, intervention times $t \leq t_1 < \dots < t_{n_{\max}} < T$ are any sequence of (\mathcal{F}_t) -stopping times, associated with a corresponding sequence of random variables $(\eta_n)_{n \leq n_{\max}}$ denoting the impulse values, with each

252 η_n being \mathcal{F}_{t_n} -measurable, for all t_n . We denote by \mathcal{Z} the set of admissible impulse values, and by \mathcal{A}
 253 the set of admissible impulse controls. For use later in the paper, we denote by $\mathcal{C}_t^* = (\{t_n, \eta_n^*\})_{n \leq n_{\max}}$,
 254 $n_{\max} \leq \infty$, the optimal impulse control.

255 In our context, the intervention time t_n correspond to the re-balancing times of the portfolio,
 256 and the impulse η_n corresponds to readjusting the amounts of the stock and bond in the investor's
 257 portfolio at time t_n . Recalling definition (2.5), t_n can formally be *any* (\mathcal{F}_t)-stopping time. However,
 258 in any numerical implementation, we are of course limited to a finite set of pre-specified potential
 259 intervention⁴ times (see for example equation (3.7) below). In what follows, we will consider both
 260 "continuous rebalancing" - see Section 5.2 (where, as $\max_n (t_n - t_{n-1}) \rightarrow 0$, we recover the ability
 261 to intervene as per definition (2.5)), as well as "discrete rebalancing", where the set of potential
 262 intervention times remain fixed - see Section 4.4.

263 The dynamics of portfolio rebalancing is as follows. Assume that the system is in state $x = (s, b)$
 264 at time t_n^- . We denote by $(S^+(t_n), B^+(t_n)) \equiv (S^+(s, b, \eta_n), B^+(s, b, \eta_n))$ the state of the system
 265 immediately after application of the impulse η_n at time t_n . More specifically, we assume that fixed
 266 and proportional transaction costs, respectively denoted by $c_1 > 0$ and c_2 , where $c_2 \in [0, 1]$, may be
 267 imposed on each rebalancing of the portfolio. Applying the impulse η_n at time t_n results in

$$268 \quad \begin{aligned} B^+(t_n) &\equiv B^+(s, b, \eta_n) = \eta_n, \\ 269 \quad S^+(t_n) &\equiv S^+(s, b, \eta_n) = (s + b) - \eta_n - c_1 - c_2 |S^+(s, b, \eta_n) - s|, \end{aligned} \quad (2.6)$$

270 where the transaction costs have been taken into account.

271 Between intervention times, for $t \in [t_n^+, t_{n+1}^-]$, the amounts S and B evolve according to the
 272 dynamics specified in (2.4) and (2.3), respectively. Specifically,

$$273 \quad \begin{aligned} \frac{dS(t)}{S(t^-)} &= (\mu - \lambda\kappa) dt + \sigma dZ + d \left(\sum_{i=1}^{\pi[t_n^+, t_{n+1}^-]} (\xi_i - 1) \right), \\ 274 \quad dB(t) &= \mathcal{R}(B(t)) B(t) dt, \quad t \in [t_n^+, t_{n+1}^-], \quad n = 0, 1, 2, \dots, n_{\max} - 1, \end{aligned} \quad (2.7)$$

275 where $\pi[t_n^+, t_{n+1}^-]$ denotes the number of jumps in the Poisson process $\pi(t)$ in the time interval
 276 $[t_n^+, t_{n+1}^-]$.

277 2.3 Admissible portfolios

278 To include transaction costs, the liquidation value $W(t)$ of the portfolio is defined to be

$$279 \quad W(t) = W(s, b) = b + \max[(1 - c_2)s - c_1, 0], \quad t \in [0, T]. \quad (2.8)$$

280 We strictly enforce two investment constraints on the *joint* values of S and B , namely a solvency
 281 condition and a maximum leverage condition. The solvency condition takes the following form: if
 282 insolvent, defined to be the case when $W(s, b) \leq 0$, we require that the position in the risky asset
 283 be liquidated, the total remaining wealth be placed in the risk-free asset, and the ceasing of all
 284 subsequent trading activities. More formally, we define a solvency region \mathcal{N} and an insolvency or
 285 bankruptcy region \mathcal{B} as follows:

$$286 \quad \mathcal{N} = \{(s, b) \in \Omega^\infty : W(s, b) > 0\}, \quad (2.9)$$

$$287 \quad \mathcal{B} = \{(s, b) \in \Omega^\infty : W(s, b) \leq 0\}, \quad (2.10)$$

⁴As is evident from Algorithm 3.1, the investor is not forced to rebalance the portfolio at a potential intervention time t_n , but can retain existing investments unchanged if it is optimal to do so, which is equivalent to "non-intervention".

288 where

$$289 \quad \Omega^\infty = [0, \infty) \times (-\infty, \infty). \quad (2.11)$$

290 The solvency condition can then be stated as

$$291 \quad \text{If } (s, b) \in \mathcal{B} \text{ at } t_n^- \quad \Rightarrow \quad \begin{cases} \text{we require } (S^+(t_n) = 0, B^+(t_n) = W(s, b)), \\ \text{and remains so for } \forall t \in [t_n, T]. \end{cases} \quad (2.12)$$

292 The investors net debt then accumulates at the borrowing rate. It is noted that due to the S -dynamics
293 (2.3), the wealth can jump into the bankruptcy region (regardless of whether we trade continuously
294 or not).

295 We also constrain the leverage ratio, i.e. at each intervention time t_n , the investor must select an
296 allocation satisfying

$$297 \quad \frac{S^+(t_n)}{S^+(t_n) + B^+(t_n)} < q_{\max} \quad (2.13)$$

298 for some positive constant q_{\max} , typically in the range $[1.0, 2.0]$.

299 2.4 Mean-variance (MV) optimization

300 Let $E_{\mathcal{C}_t}^{x,t}[W(T)]$ and $Var_{\mathcal{C}_t}^{x,t}[W(T)]$ denote the mean and variance of the liquidation value of the
301 terminal wealth, respectively, given the state $x = (s, b)$ at time t and using impulse control $\mathcal{C}_t \in \mathcal{A}$
302 over $[t, T]$.

303 2.4.1 Pre-commitment

304 Using the standard linear scalarization method for multi-criteria optimization problems (Yu, 1971),
305 we define the (time- t) *pre-commitment MV* (PCMV) problem by

$$306 \quad (PCMV_t(\rho)) : \quad \sup_{\mathcal{C}_t \in \mathcal{A}} \left(E_{\mathcal{C}_t}^{x,t}[W(T)] - \rho Var_{\mathcal{C}_t}^{x,t}[W(T)] \right), \quad \rho > 0. \quad (2.14)$$

307 Here, the scalarization parameter ρ reflects the investor's level of risk aversion. The MV "efficient
308 frontier" is defined as the following set of points in \mathbb{R}^2 :

$$309 \quad \left\{ \left(\sqrt{Var_{\mathcal{C}_0^*}^{x_0,0}[W(T)]}, E_{\mathcal{C}_0^*}^{x_0,0}[W(T)] \right) : \rho > 0 \right\}, \quad (2.15)$$

310 traced out by solving (2.14) for each $\rho > 0$. In other words, given a fixed level of risk aversion, an
311 "efficient" portfolio, i.e. any point in the set (2.15), cannot be improved upon in the MV sense, using
312 any other admissible strategy in \mathcal{A} .

313 There are two important issues related to the pre-commitment MV problem (2.14). First, since
314 variance does not satisfy the smoothing property of conditional expectation, dynamic programming
315 cannot be used directly to solve (2.14). To overcome this challenge, an embedding approach for solving
316 (2.14) is proposed in Li and Ng (2000); Zhou and Li (2000) - see Dang and Forsyth (2014); Dang et al.
317 (2016); Wang and Forsyth (2010) for the numerical treatment of the problem as well as a discussion
318 of technical issues.

319 The second issue is the "time-inconsistency" of the resulting optimal control (see Bjork et al.
320 (2016); Bjork and Murgoci (2014)). To this end, with a slight abuse of notation, we denote by $\mathcal{C}_{t,u}^*$
321 the optimal control for problem $PCMV_t(\rho)$ computed at time t for a fixed time $u \in [t, T]$. For the
322 pre-commitment approach, the "time-inconsistency" phenomenon means that, in general,

$$323 \quad \mathcal{C}_{t,u}^* \neq \mathcal{C}_{t',u}^*, \quad t' > t, \quad u \in [t', T]. \quad (2.16)$$

324 However, we note that the issue of time-inconsistency is, to some extent, a matter of perspective. This
 325 is because it can be shown that problem (2.14) is equivalent to target-based optimization, where a
 326 quadratic loss function is minimized - see Vigna (2014). From this perspective, for a fixed target, the
 327 optimal control *is* time consistent, but it remains time-inconsistent when viewed from the perspective
 328 of the original problem (2.14).

329 2.4.2 Time-consistent approach

330 In contrast, the *time-consistent MV* (TCMV) optimization problem - first studied in Basak and
 331 Chabakauri (2010) and later substantially expanded and generalized in Bjork et al. (2016); Bjork and
 332 Murgoci (2014); Hu et al. (2012) - enforces equality, instead of inequality, in (2.16). Specifically, a
 333 “time-consistency constraint” is imposed on (2.14), and this gives the time-consistent MV (TCMV)

$$334 \quad (TCMV_t(\rho)) : \quad V(s, b, t) = \sup_{C_t \in \mathcal{A}} \left(E_{C_t}^{x,t} [W(T)] - \rho \text{Var}_{C_t}^{x,t} [W(T)] \right), \quad (2.17)$$

$$335 \quad \text{s. t.} \quad C_{t,u}^* = C_{t',u}^*, \quad \text{for all } t' \geq t \text{ and } u \geq t'. \quad (2.18)$$

336 Dynamic programming can be applied directly to (2.17)-(2.18) to compute optimal controls and the
 337 TCMV efficient frontier. See, for example Wang and Forsyth (2011), for the pure-diffusion case.

338 Since the constrained optimization problem (2.17)-(2.18) always leads to MV outcomes inferior to,
 339 or at most, the same as, those of the unconstrained optimization problem (2.14), a natural question is:
 340 what makes time-consistent MV optimization potentially attractive? As discussed in the introduction,
 341 the pre-commitment approach may not be feasible in institutional settings, while, on the contrary,
 342 the time-consistent approach is typically popular in these settings. However, it should be noted that
 343 neither the pre-commitment nor the time-consistent approach is “better” in some objective sense - see
 344 Vigna (2016, 2017) for a discussion of a number of subtle issues involved.

345 *Remark 2.1.* (Game-theoretic perspective; notion of optimality). In Bjork and Murgoci (2014), the
 346 terminology “equilibrium” control is used as opposed to “optimal” control, since the time-consistent
 347 optimal control C_t^* satisfies the conditions of a subgame perfect Nash equilibrium control. We will
 348 follow the example of Basak and Chabakauri (2010); Cong and Oosterlee (2016); Li and Li (2013);
 349 Wang and Forsyth (2011) and retain the terminology “optimal” (time-consistent) control for simplicity.

350 3 Algorithm development

351 For subsequent use, we write the value function $V(s, b, t)$ of the time-consistent problem (2.17)-(2.18)
 352 in terms of two auxiliary functions $U(s, b, t)$ and $Q(s, b, t)$ as follows

$$353 \quad V(s, b, t) = U(s, b, t) - \rho Q(s, b, t) + \rho(U(s, b, t))^2, \quad (3.1)$$

354 where

$$355 \quad U(s, b, t) = E_{C_t^*}^{x,t} [W(T)], \quad (3.2)$$

$$356 \quad Q(s, b, t) = E_{C_t^*}^{x,t} \left[(W(T))^2 \right], \quad (3.3)$$

357 where, it is implicitly understood hereafter that C_t^* is the optimal control for the $TCMV_t(\rho)$ problem.
 358 We also define the following operators, applied to an appropriate test function f :

$$359 \quad \mathcal{L}f(s, b, t) = (\mu - \lambda\kappa) s f_s + \mathcal{R}(b) b f_b + \frac{1}{2} \sigma^2 s^2 f_{ss} - \lambda f, \quad (3.4)$$

$$360 \quad \mathcal{J}f(s, b, t) = \lambda \int_0^\infty f(\xi s, b, t) p(\xi) d\xi. \quad (3.5)$$

361 We now primarily focus on the continuous re-balancing case. The discrete rebalancing case is discussed
 362 in Subsection (4.4).

363 Fix an arbitrary point in time $t \in [0, T]$, and assume we are in state $x = (s, b)$ at time t^- . We
 364 define the intervention operator, a fundamental object in impulse control problems (Oksendal and
 365 Sulem, 2005), applied to the value function V of the time-consistent problem (2.17)-(2.18) as

$$366 \quad \mathcal{M}V(s, b, t) = \sup_{\eta \in \mathcal{Z}} [V(S^+(s, b, \eta), B^+(s, b, \eta), t)], \quad (3.6)$$

367 where $S^+(\cdot)$ and $B^+(\cdot)$ are defined in (2.6).

368 In analogy to the case of continuous controls, where an extended HJB system of equations is
 369 obtained (see Bjork et al. (2016)), as discussed in the Introduction, in our case, the techniques of
 370 Bjork et al. (2016); Bjork and Murgoci (2014) results in an extended HJB quasi-integrovariational
 371 inequality - a strongly coupled, nonlinear system of equations that needs to solve simultaneously to
 372 obtain the value function. Under realistic modelling assumptions and investment constraints, a closed-
 373 form solution for this highly complex system of equations is not known to exist, except for very special
 374 cases, and hence a numerical method must be used. However, it is not clear how such a highly complex
 375 system of equations can be solved effectively numerically for practical purposes.

376 To overcome the above-mentioned hurdle, we choose to enforce the dynamic programming principle
 377 on the discretized time variable, i.e. the time-consistency constraint (2.18) is enforced on a set of
 378 discrete intervention times obtained from discretizing the time variable. The intervention operator
 379 \mathcal{M} , defined in (3.6), is applied across each of these times. As shown later, this approach results in only
 380 linear partial integro-differential equations to solve between intervention times. Furthermore, when
 381 combined with a semi-Lagrangian timestepping scheme, we just have a set of one-dimensional PIDE
 382 in the s -variable to solve between intervention times. As a result, our approach is not only numerically
 383 simpler than the approach of Bjork et al. (2016); Bjork and Murgoci (2014), but also computationally
 384 effective.

385 3.1 Recursive relationships

386 We consider the following uniform partition of the time interval $[0, T]$

$$387 \quad \mathcal{T}_{n_{\max}} = \{t_n \mid t_n = n\Delta t\}, \quad \Delta t = T/n_{\max}, \quad \Delta t = C_1 h, \quad (3.7)$$

388 where C_1 is positive and independent of the discretization parameter $h > 0$. In the limit as $h \rightarrow 0$,
 389 we shall demonstrate via numerical experiments that, at least for some known cases, the numerical
 390 solution of the time-discretized formulation converges to the closed-form solution of the continuous
 391 time formulation.

392 To avoid heavy notation, we now introduce the following notational convention: any admissible
 393 impulse control $\mathcal{C} \in \mathcal{A}$ will be written as the set of impulses

$$394 \quad \mathcal{C} = \{\eta_n \in \mathcal{Z} : n = 0, \dots, n_{\max}\}, \quad (3.8)$$

395 where the corresponding set of (discretized) intervention times is implicitly understood to be $\{t_n\}_{n=0}^{n_{\max}}$.
 396 Given an impulse control \mathcal{C} as in (3.8), we also define the control $\mathcal{C}_n \equiv \mathcal{C}_{t_n} \subseteq \mathcal{C}$, $n = 0, \dots, n_{\max}$, as
 397 the subset of impulses (and, implicitly, corresponding intervention times) of \mathcal{C} applicable to the time
 398 interval $[t_n, T]$:

$$399 \quad \mathcal{C}_n = \{\eta_n, \dots, \eta_{n_{\max}}\} \subseteq \mathcal{C} = \{\eta_0, \dots, \eta_{n_{\max}}\}. \quad (3.9)$$

400 Subsequently, we use

$$401 \quad \mathcal{C}_n^* = \{\eta_n^*, \dots, \eta_{n_{\max}}^*\} \quad (3.10)$$

402 to denote the optimal impulse control to the problem $(TCMV_{t_n}(\rho))$ defined in (2.17)-(2.18).

403 With this time discretization and notational conventions, for a given scalarization parameter $\rho > 0$
 404 and an intervention time t_n , we define the scalarized time-consistent MV problem $(TCMV_{t_n}(\rho))$ as
 405 follows:

$$406 \quad (TCMV_{t_n}(\rho)) : \quad V(s, b, t_n) = \sup_{\mathcal{C}_n \in \mathcal{A}} \left(E_{\mathcal{C}_n}^{x, t_n} [W(T)] - \rho \text{Var}_{\mathcal{C}_n}^{x, t_n} [W(T)] \right) \quad (3.11)$$

$$407 \quad \text{s.t. } \mathcal{C}_n = \{\eta_n, \mathcal{C}_{n+1}^*\} := \{\eta_n, \eta_{n+1}^*, \dots, \eta_{n_{\max}-1}^*, \eta_{n_{\max}}^*\} \quad (3.12)$$

408 where \mathcal{C}_{n+1}^* is optimal for problem $(TCMV_{t_{n+1}}(\rho))$.

409 We note that the definition of (3.11)-(3.12) agrees conceptually with the continuous-time definition
 410 given by (2.17)-(2.18), but is more convenient from a computational perspective. The particular form
 411 of the time-consistency constraint in (3.12) is a discretized equivalent of the constraint in (2.18), since,
 412 given the optimal impulse control $\mathcal{C}_{n+1}^* = \{\eta_{n+1}^*, \dots, \eta_{n_{\max}}^*\}$ of problem $(TCMV_{t_{n+1}}(\rho))$ applicable
 413 to the time period $[t_{n+1}, T]$, any *arbitrary* admissible impulse control $\mathcal{C}_n \in \mathcal{A}$ will necessarily be of the
 414 form

$$415 \quad \mathcal{C}_n = \{\eta, \eta_{n+1}^*, \dots, \eta_{n_{\max}}^*\} = \{\eta, \mathcal{C}_{n+1}^*\} \quad (3.13)$$

416 for some admissible impulse value $\eta \in \mathcal{Z}$ applied at time t_n .

417 We use the notation $E_{\eta}^{x, t_n}[\cdot]$ to indicate that the expectation is evaluated using an (arbitrary)
 418 impulse value $\eta \in \mathcal{Z}$ at time t_n , with the implied application of \mathcal{C}_{n+1}^* over the time interval $[t_{n+1}, T]$.
 419 We note that, given $X(t_{n+1}^-) = (S(t_{n+1}^-), B(t_{n+1}^-))$ at time t_{n+1}^- , we have the following recursive
 420 relationships for $U(s, b, t_n)$ and $Q(s, b, t_n)$:

$$421 \quad U(s, b, t_n) = E_{\eta_n^*}^{x, t_n} [U(S(t_{n+1}^-), B(t_{n+1}^-), t_{n+1})], \quad (3.14)$$

$$422 \quad Q(s, b, t_n) = E_{\eta_n^*}^{x, t_n} [Q(S(t_{n+1}^-), B(t_{n+1}^-), t_{n+1})], \quad (3.15)$$

423 where, as defined previously in (3.10), η_n^* is the optimal impulse value for time t_n . For the special case
 424 of $t_{n_{\max}} = T$, we have

$$425 \quad U(s, b, T) = U(s, b, t_{n_{\max}}) = W(s, b), \quad (3.16)$$

$$426 \quad Q(s, b, T) = Q(s, b, t_{n_{\max}}) = (W(s, b))^2. \quad (3.17)$$

427 We similarly obtain a recursive relationship for the value function (3.11)

$$428 \quad V(s, b, t_n) = \sup_{\eta \in \mathcal{Z}} \left\{ E_{\eta}^{x, t_n} [U(S(t_{n+1}^-), B(t_{n+1}^-), t_{n+1})] - \rho E_{\eta}^{x, t_n} [Q(S(t_{n+1}^-), B(t_{n+1}^-), t_{n+1})] \right. \\ 429 \quad \left. + \rho (E_{\eta}^{x, t_n} [U(S(t_{n+1}^-), B(t_{n+1}^-), t_{n+1})])^2 \right\}, \quad (3.18)$$

430 where, for the special case of $t_{n_{\max}}$, we have $V(s, b, t_{n_{\max}}) = V(s, b, T) = W(s, b)$. This is effectively
 431 the discretized version of the intervention operator \mathcal{M} , defined in (3.6).

432 Assume that $E_{\eta}^{x, t_n}[\cdot]$ is a bounded, upper semi-continuous function of the admissible impulse value
 433 η . If we can determine $U(S(t_{n+1}^-), B(t_{n+1}^-), t_{n+1})$ and $Q(S(t_{n+1}^-), B(t_{n+1}^-), t_{n+1})$, then

$$434 \quad \eta_n^* \in \arg \max_{\eta \in \mathcal{Z}} \left\{ E_{\eta}^{x, t_n} [U(S(t_{n+1}^-), B(t_{n+1}^-), t_{n+1})] - \rho E_{\eta}^{x, t_n} [Q(S(t_{n+1}^-), B(t_{n+1}^-), t_{n+1})] \right. \\ 435 \quad \left. + \rho (E_{\eta}^{x, t_n} [U(S(t_{n+1}^-), B(t_{n+1}^-), t_{n+1})])^2 \right\}. \quad (3.19)$$

436 Relations (3.14)-(3.19) form the basis for a recursive algorithm to determined the value function and
 437 the optimal impulse value.

3.2 Computation of expectations

We now introduce the change of variable $\tau = T - t$, and let

$$\bar{U}(s, b, \tau) = U(s, b, T - t), \quad \bar{Q}(s, b, \tau) = Q(s, b, T - t), \quad \bar{V}(s, b, \tau) = V(s, b, T - t), \quad (3.20)$$

and hence (3.1) becomes

$$\bar{V}(s, b, \tau) = \bar{U}(s, b, \tau) - \rho \bar{Q}(s, b, \tau) + \rho (\bar{U}(s, b, \tau))^2 \quad (3.21)$$

In terms of τ , time grid (3.7) now becomes

$$\{\tau_n = T - t_{n_{\max} - n} : n = 0, 1, \dots, n_{\max}\}. \quad (3.22)$$

Next, we define the following ‘‘candidate’’ expectation values at the rebalancing time τ_n under an arbitrary impulse $\eta \in \mathcal{Z}$:

$$\hat{U}_\eta^n(s, b) = E_\eta^{x, \tau_n} [\bar{U}(S(\tau_{n-1}^+), B(\tau_{n-1}^+), \tau_{n-1}^+)], \quad (3.23)$$

$$\hat{Q}_\eta^n(s, b) = E_\eta^{x, \tau_n} [\bar{Q}(S(\tau_{n-1}^+), B(\tau_{n-1}^+), \tau_{n-1}^+)]. \quad (3.24)$$

To handle the computation of expectations in (3.23) and (3.24), we proceed as follows. For solvent portfolios, i.e. $(s, b) \in \mathcal{N}$, we first solve the following associated two PIDEs from τ_{n-1}^+ to τ_n^- (Oksendal and Sulem, 2005)

$$\Psi_\tau(s, b, \tau) - \mathcal{L}\Psi(s, b, \tau) - \mathcal{J}\Psi(s, b, \tau) = 0 \quad (s, b, \tau) \in \mathcal{N} \times (\tau_{n-1}^+, \tau_n^-] \quad (3.25)$$

$$\text{with initial condition } \Psi(s, b, \tau_{n-1}^+) = \bar{U}(s, b, \tau_{n-1}) \quad (3.26)$$

and

$$\Phi_\tau(s, b, \tau) - \mathcal{L}\Phi(s, b, \tau) - \mathcal{J}\Phi(s, b, \tau) = 0 \quad (s, b, \tau) \in \mathcal{N} \times (\tau_{n-1}^+, \tau_n^-] \quad (3.27)$$

$$\text{with initial condition } \Phi(s, b, \tau_{n-1}^+) = \bar{Q}(s, b, \tau_{n-1}) \quad (3.28)$$

where, for the special case of $\tau_0 = 0$, we have

$$\bar{U}(s, b, 0) = W(s, b), \quad \bar{Q}(s, b, 0) = (W(s, b))^2. \quad (3.29)$$

Here, the operators \mathcal{L} and \mathcal{J} in the PDEs (3.25) and (3.27) are defined in (3.4) and (3.5), respectively. Then, for a given arbitrary impulse $\eta \in \mathcal{Z}$, we obtain the ‘‘candidate’’ expectation values $\hat{U}_\eta^n(s, b)$ and $\hat{Q}_\eta^n(s, b)$ by

$$\hat{U}_\eta^n(s, b) = \Psi(S(\tau_n^+), B(\tau_n^+), \tau_n^-), \quad (3.30)$$

$$\hat{Q}_\eta^n(s, b) = \Phi(S(\tau_n^+), B(\tau_n^+), \tau_n^-), \quad (3.31)$$

where $B(\tau_n^+) = \eta$ and $S(\tau_n^+) = (s + b) - \eta - c_1 - c_2 \cdot |S(\tau_n^+) - s|$, as per (2.6), subject to the leverage constraint (2.13). Finally, using (3.30)-(3.31), we can find the optimal impulse value η_n^* via

$$\eta_n^* \in \arg \max_{\eta \in \mathcal{Z}} \left\{ \hat{U}_\eta^n(s, b) - \rho \hat{Q}_\eta^n(s, b) + \rho (\hat{U}_\eta^n(s, b))^2 \right\}.$$

For insolvent portfolios, i.e. $(s, b) \in \mathcal{B}$, the solvency constraint (2.12) results in enforced liquidation. This is captured by a Dirichlet condition

$$\begin{aligned} \bar{U}(s, b, \tau_n^-) &= \bar{U}(0, W(s, b)e^{\mathcal{R}(s+b)\tau_n}, 0), \\ \bar{Q}(s, b, \tau_n^-) &= \bar{Q}(0, W(s, b)e^{\mathcal{R}(s+b)\tau_n}, 0), \quad (s, b) \in \mathcal{B}. \end{aligned} \quad (3.32)$$

In Algorithm 3.1, we present a recursive algorithm for the time-consistent MV ($TCMV_n(\rho)$) for a fixed $\rho > 0$.

Algorithm 3.1 Recursive algorithm to solve $(TCMV_n(\rho))$ for a fixed $\rho > 0$.

```

1: set  $\bar{U}(s, b, 0) = W(s, b)$  and  $\bar{Q}(s, b, 0) = (W(s, b))^2$ ;
2: for  $n = 1, \dots, n_{\max}$  do
3:   if  $(s, b) \in \mathcal{B}$  then
4:     enforce the solvency constraint (2.12) via (3.32) to obtain  $\bar{U}(s, b, \tau_n)$  and  $\bar{Q}(s, b, \tau_n)$ ;
5:   else
6:     solve (3.25)-(3.26) and (3.27)-(3.28) from  $\tau_{n-1}^+$  to  $\tau_n^-$  to obtain  $\Psi(s, b, \tau_n^-)$  and  $\Phi(s, b, \tau_n^-)$ ;
7:     for each  $\eta \in \mathcal{Z}$  do
8:       set  $B^+ = \eta$  and  $S^+ = s + b - \eta - c_1 - c_2 \cdot |S^+ - s|$  as per (2.6), subject to the leverage
       constraint (2.13);
9:       compute  $\hat{U}_\eta^n(s, b) = \Psi(S^+, B^+, \tau_n^-)$  and  $\hat{Q}_\eta^n(s, b) = \Phi(S^+, B^+, \tau_n^-)$ ;
10:    end for
11:    find  $\eta_n^* \in \arg \max_{\eta \in \mathcal{Z}} \left\{ \hat{U}_\eta^n(s, b) - \rho \hat{Q}_\eta^n(s, b) + \rho \left( \hat{U}_\eta^n(s, b) \right)^2 \right\}$ ;
12:    set  $\bar{U}(s, b, \tau_n) = \hat{U}_{\eta_n^*}^n(s, b)$  and  $\bar{Q}(s, b, \tau_n) = \hat{Q}_{\eta_n^*}^n(s, b)$ ;
13:  end if
14: end for
15: return  $V(s, b, \tau_{n_{\max}}) = \bar{U}(s, b, \tau_{n_{\max}}) - \rho \bar{Q}(s, b, \tau_{n_{\max}}) + \rho (\bar{U}(s, b, \tau_{n_{\max}}))^2$ ;

```

473 *Remark 3.1.* (Convergence of numerical solution). Since the viscosity solution theory (Crandall et al.
474 (1992)) does not apply in this case, we have no proof that Algorithm 3.1 converges to an appropriately
475 defined (weak) solution of the corresponding extended HJB quasi-integrovariational inequality in the
476 limit as $\Delta\tau \rightarrow 0$. However, we can show, as in Cong and Oosterlee (2016); Wang and Forsyth (2011),
477 that our numerical solution converges to known analytical solutions available in special cases. Where
478 no analytical solutions are available, the numerical PDE results are validated using Monte Carlo
479 simulation.

480 4 Localization

481 4.1 Semi-Lagrangian timestepping scheme

482 Recall the definition of the operator \mathcal{L} , defined in (3.4). We observe that the PIDEs (3.25) and
483 (3.27) for $\Psi(s, b, \tau)$ and $\Phi(s, b, \tau)$, respectively, that need to be solved in Step 6 in Algorithm 3.1.
484 involves partial derivatives with respect to both s and b . Direct implementation would be therefore
485 computationally expensive.

486 With this in mind, we introduce the semi-Lagrangian timestepping scheme proposed in Dang and
487 Forsyth (2014). The intuition behind the the semi-Lagrangian timestepping scheme is that, instead of
488 obtaining the PIDEs by modelling the change (via Ito's lemma) in a test function $f(S(\tau), B(\tau), \tau)$
489 with both S and B varying, we consider the Lagrangian derivative along the trajectory where B is
490 held fixed over the length of the timestep. Specifically, we model the change in $f(S(\tau), B(\tau), \tau)$ with
491 $(S(\tau), B(\tau) = b)$ for $\tau \in [\tau_{n-1}^+, \tau_n^-]$, with interest paid only at the end of the timestep, i.e. at time
492 τ_n , at which time the amount in the risk-free asset would jump to $b \cdot \exp\{\mathcal{R}(b) \Delta\tau\}$, reflecting the
493 settlement (payment or receipt) of interest due for the time interval $[\tau_{n-1}, \tau_n]$. Along this trajectory,
494 the partial derivative of the test function $f(s, b, \tau)$ with respect to the b -variable is zero, resulting in
495 a decoupling of the PIDE for every value of the b -variable.

496 We emphasize that the above argument is an intuitive explanation of the semi-Lagrangian scheme.
497 In fact, we can prove rigorously that in the limit as $\Delta\tau \rightarrow 0$, this treatment converges to the case

498 where interest is paid continuously.⁵ Moreover, this approach is also valid for discrete rebalancing,
 499 regardless of whether the interest is paid continuously or discretely.

500 Applying this reasoning to the two PIDEs (3.25) and (3.27), we have

$$501 \quad \Psi_b(s, b, \tau) = \Phi_b(s, b, \tau) = 0, \quad (s, b, \tau) \in \mathcal{N} \times (\tau_{n-1}^+, \tau_n^-],$$

502 and we can replace the operator \mathcal{L} in the PDEs (3.25) and (3.27) by the operator \mathcal{P} defined as

$$503 \quad \mathcal{P}f(s, b, t) = (\mu - \lambda\kappa)sf_s + \frac{1}{2}\sigma^2s^2f_{ss} - \lambda f. \quad (4.1)$$

504 Therefore, instead of solving a *two*-dimensional PDE in space variables (s, b) for both Ψ and Φ , we
 505 now solve, for each discrete value of b , two *one*-dimensional PIDEs (in a single space variable s):

$$506 \quad \begin{aligned} \Psi_\tau(s, b, \tau) - \mathcal{P}\Psi(s, b, \tau) - \mathcal{J}\Psi(s, b, \tau) &= 0, & (s, b, \tau) \in \mathcal{N} \times (\tau_{n-1}^+, \tau_n^-] \\ \text{with initial condition } \Psi(s, b, \tau_{n-1}^+) &= \bar{U}(s, b, \tau_{n-1}), \end{aligned} \quad (4.2)$$

508 and

$$509 \quad \begin{aligned} \Phi_\tau(s, b, \tau) - \mathcal{P}\Phi(s, b, \tau) - \mathcal{J}\Phi(s, b, \tau) &= 0, & (s, b, \tau) \in \mathcal{N} \times (\tau_{n-1}^+, \tau_n^-] \\ \text{with initial condition } \Phi(s, b, \tau_{n-1}^+) &= \bar{Q}(s, b, \tau_{n-1}). \end{aligned} \quad (4.3)$$

511 The second consequence of semi-Lagrangian timestepping is that the calculation of the value of
 512 $S(\tau_n^-)$, used in computing $\hat{U}_\eta^n(s, b)$ and $\hat{Q}_\eta^n(s, b)$ as per (3.30) and (3.31), has to be adjusted to reflect
 513 the payment of interest at time τ_n :

$$514 \quad S(\tau_n^+) = \left(s + be^{\mathcal{R}(b)\Delta\tau}\right) - \eta - c_1 - c_2 \cdot |S(\tau_n^+) - s|. \quad (4.4)$$

515 4.2 Localization

516 Each set of PIDEs (4.2) - (4.3), together with the Dirichlet conditions (3.32), are to be solved in the
 517 domain $(s, b, \tau) \in \Omega^\infty \equiv [0, \infty) \times (-\infty, +\infty) \times [\tau_{n-1}^+, \tau_n^-]$. For computational purposes, we localize this
 518 domain to the set of points

$$519 \quad (s, b, \tau) \in \Omega \times [\tau_{n-1}^+, \tau_n^-] = [0, s_{\max}) \times [-b_{\max}, b_{\max}] \times [\tau_{n-1}^+, \tau_n^-],$$

520 where s_{\max} and b_{\max} are sufficiently large positive numbers. Let $s^* < s_{\max}$. Following Dang and
 521 Forsyth (2014), we define the following sub-computational domains

$$522 \quad \Omega_{s^*} = (s^*, s_{\max}] \times [-b_{\max}, b_{\max}], \quad (4.5)$$

$$523 \quad \Omega_{s_0} = \{0\} \times [-b_{\max}, b_{\max}], \quad (4.6)$$

$$524 \quad \Omega_{\mathcal{B}} = \{(s, b) \in \Omega \setminus \Omega_{s^*} \setminus \Omega_{s_0} : W(s, b) \leq 0\}, \quad (4.7)$$

$$525 \quad \Omega_{in} = \Omega \setminus \Omega_{s^*} \setminus \Omega_{s_0} \setminus \Omega_{\mathcal{B}}, \quad (4.8)$$

$$526 \quad \Omega_{b_{\max}} = (0, s^*] \times [-b_{\max}e^{r_{\max}T}, -b_{\max}) \cup (b_{\max}, b_{\max}e^{r_{\max}T}], \quad (4.9)$$

527 where $r_{\max} = \max(r_b, r_\ell)$. Following the steps in Dang and Forsyth (2014), we have the following
 528 localized problem for Ψ :

$$529 \quad \begin{aligned} \Psi_\tau(s, b, \tau) - \mathcal{P}\Psi(s, b, \tau) - \mathcal{J}_\ell\Psi(s, b, \tau) &= 0, & (s, b, \tau) \in \Omega_{in} \times [\tau_{n-1}^+, \tau_n^-], \\ \Psi_\tau(s, b, \tau) - \mu\Psi(s, b, \tau) &= 0, & (s, b, \tau) \in \Omega_{s^*} \times [\tau_{n-1}^+, \tau_n^-], \\ \Psi(s, b, \tau) - U(0, b, \tau_{n-1}) &= 0, & (s, b, \tau) \in \Omega_{s_0} \times [\tau_{n-1}^+, \tau_n^-], \\ \Psi(s, |b| > |b_{\max}|, \tau) - \frac{|b|}{b_{\max}}\Psi(s, \text{sgn}(b)b_{\max}, \tau) &= 0, & (s, b, \tau) \in \Omega_{b_{\max}} \times [\tau_{n-1}^+, \tau_n^-], \\ \text{with } \Psi(s, b, \tau = \tau_{n-1}) - U(s, b, \tau_{n-1}) &= 0, & (s, b) \in \Omega. \end{aligned} \quad (4.10)$$

⁵See Dang and Forsyth (2014) for the consistency proof in the context of the pre-commitment mean-variance problem.

534 while the localized problem for Φ is as follows:

$$\begin{aligned}
535 \quad & \Phi_\tau(s, b, \tau) - \mathcal{P}\Phi(s, b, \tau) - \mathcal{J}_\ell\Phi(s, b, \tau) = 0, \quad (s, b, \tau) \in \Omega_{in} \times [\tau_{n-1}^+, \tau_n^-] \\
536 \quad & \Phi_\tau(s, b, \tau) - [2\mu + \sigma^2 + \lambda\kappa_2]\Phi(s, b, \tau) = 0, \quad (s, b, \tau) \in \Omega_{s^*} \times [\tau_{n-1}^+, \tau_n^-], \\
537 \quad & \Phi(s, b, \tau) - Q(0, b, \tau_{n-1}) = 0, \quad (s, b, \tau) \in \Omega_{s_0} \times [\tau_{n-1}^+, \tau_n^-], \\
538 \quad & \Phi(s, |b| > |b_{\max}|, \tau) - \left(\frac{b}{b_{\max}}\right)^2 \Phi(s, \text{sgn}(b) b_{\max}, \tau) = 0, \quad (s, b, \tau) \in \Omega_{b_{\max}} \times [\tau_{n-1}^+, \tau_n^-] \\
539 \quad & \text{with } \Phi(s, b, \tau = \tau_{n-1}) - Q(s, b, \tau_{n-1}) = 0, \quad (s, b) \in \Omega. \tag{4.11}
\end{aligned}$$

540 Here,

$$541 \quad \mathcal{J}_\ell f(s, b, \tau) = \lambda \int_0^{s_{\max}/s} f(\xi s, b, \tau) p(\xi) d\xi, \tag{4.12}$$

542 We note that the problem is only solved in Ω . Should any values in $\Omega_{b_{\max}}$ be required, they are
543 deduced from the computed solution in Ω . Some guidelines for choosing s^* , s_{\max} which minimize the
544 effect of the localization error for the jump terms can be found in d'Halluin et al. (2005). We refer the
545 reader to Dang and Forsyth (2014) for relevant details regarding a derivation of the localized problems
546 (4.10)-(4.11).

547 We solve the localized problems (4.10)-(4.11) using finite differences as described in Dang and
548 Forsyth (2014). Specifically, in addition to the time grid in (3.22), we also introduce nodes, not nec-
549 essarily equally spaced, in the s -direction $\{s_i : i = 1, \dots, i_{\max}\}$ and b -direction $\{b_j : j = 1, \dots, j_{\max}\}$,
550 with $\Delta s_{\max} = \max_i (s_{i+1} - s_i) = C_3 h$ and $\Delta b_{\max} = \max_j (b_{j+1} - b_j) = C_4 h$, where C_3 and C_4 are posi-
551 tive and independent of h . Using the nodes in the b -direction, we define $\mathcal{Z}_h = \{b_j : j = 1, \dots, j_{\max}\} \cap \mathcal{Z}$
552 to be the discretization of the admissible impulse space. We use linear interpolation onto the computa-
553 tional grid if the spatial point $(s_i, b_j e^{\mathcal{R}(b_j)\Delta\tau})$, arising from the implementation of the semi-Lagrangian
554 timestepping scheme (see Section 4.1), does not correspond to any available grid point.

555 Central differencing is used as much as possible for the discrete approximation to the operator \mathcal{P}
556 in (4.1), but we require that the scheme be a positive coefficient method (Wang and Forsyth, 2008).
557 The operator \mathcal{J}_ℓ in (4.12) is handled using the method described in d'Halluin et al. (2005), which
558 avoids a dense matrix solve (due to the presence of the jump term) by using a fixed-point iteration to
559 solve the discrete equations arising at each b -grid node and timestep.

560 4.3 Construction of efficient frontier

561 We assume that the given initial wealth, denoted by $W(t=0) = W_{init}$, is invested in the risk-free
562 asset, so that the time $t=0$ portfolio is given by $(S(0), B(0)) = (0, W_{init})$. For initial wealth W_{init} ,
563 and given the positive discretization parameter h , the goal is the tracing out of the efficient frontier
564 using the scalarization parameter ρ :

$$565 \quad \mathcal{Y}_h = \bigcup_{\rho \geq 0} \left(\sqrt{\left(\text{Var}_{C_0^*}^{t=0} [W(T)] \right)_h}, \left(E_{C_0^*}^{t=0} [W(T)] \right)_h \right)_\rho, \tag{4.13}$$

566 where $(\cdot)_h$ refers to a discretization approximation to the expression in the brackets.

567 This can be achieved as follows. For a fixed value $\rho \geq 0$ in $\{\rho_{\min}, \dots, \rho_{\max}\} \subset [0, \infty)$, executing
568 Algorithm 3.1 gives us the following quantities:

$$569 \quad U_0(W_{init}) \simeq \left(E_{C_0^*}^{(s=0, b=W_{init}), t=0} [W(T)] \right)_h, \quad Q_0(W_{init}) \simeq \left(E_{C_0^*}^{(s=0, b=W_{init}), t=0} [(W(T))^2] \right)_h,$$

570 Using these, we compute the corresponding single point on the efficient frontier \mathcal{Y}_h (4.13):

$$571 \quad \left(\text{Var}_{C_0^*}^{t=0} [W(T)] \right)_h = Q_0(W_{init}) - (U_0(W_{init}))^2, \quad \left(E_{C_0^*}^{t=0} [W(T)] \right)_h = U_0(W_{init}). \tag{4.14}$$

572 *Remark 4.1.* (Complexity) For each timestep, we have to perform i) a local optimization problem to
573 search for the optimal impulse η_n^* at each node, and ii) a time advance step for the two PIDEs (4.10)
574 and (4.11). From the perspective of a complexity analysis, this is similar to the case encountered in
575 Dang and Forsyth (2014), with the exception that there are two PIDEs to be solved for each value of b ,
576 instead of one. As a result, the complexity analysis of Dang and Forsyth (2014) holds for the algorithm
577 described here as well. Recalling the positive discretization parameter h in (3.7), we conclude that
578 the total complexity of constructing an efficient frontier is $\mathcal{O}(1/h^5)$.

579 4.4 Discrete rebalancing

580 The formulation of the problem up to this point assumes continuous rebalancing of the portfolio
581 - equivalently, in the discretized setting, the portfolio is rebalanced at every timestep. While the
582 continuous rebalancing treatment is crucial for numerical tests showing convergence to the known
583 closed form solutions (see Section 5.2 below), it is not realistic - and in the presence of transaction
584 costs, it is also not practically feasible.

585 For the construction of efficient frontiers (see Section 5), we therefore assume discrete rebalancing.
586 That is, the portfolio is only rebalanced at a set of pre-determined intervention times $0 = \tilde{t}_0 \leq \tilde{t}_1 <$
587 $\dots < \tilde{t}_{m_{\max}} < T$, where t_0 is the inception of the investment. With the change of variable $\tau = T - t$,
588 the set of intervention times become

$$589 \quad 0 = \tilde{\tau}_0 < \tilde{\tau}_1 < \dots < \tilde{\tau}_{m_{\max}} = T, \quad m_{\max} < \infty. \quad (4.15)$$

590 Algorithm 3.1 can easily be modified to handle discrete rebalancing. Specifically, in Step 6, the PIDEs
591 (3.25)-(3.26) and (3.27)-(3.28) are solved from from $\tilde{\tau}_{m-1}^+$ to $\tilde{\tau}_m^-$, $m = 1, \dots, m_{\max}$, possibly using
592 multiple timesteps for the solution of the corresponding PIDE, to obtain $\Psi(s, b, \tilde{\tau}_m^-)$ and $\Phi(s, b, \tilde{\tau}_m^-)$.
593 Other steps of the algorithm remain unchanged. In this case, the complexity of the algorithm for
594 constructing the entire efficient frontier is $\mathcal{O}(1/h^4 |\log h|)$.

595 5 Numerical results

596 5.1 Empirical data and calibration

597 In order to obtain the required process parameters, the same data and calibration technique is used
598 as in Dang and Forsyth (2016); Forsyth and Vetzal (2017). The empirical data sources are as follows:

- 599 • Risky asset data: Daily total return data covering the period *1926:1 - 2014:12* - which includes
600 dividends and other distributions - from the Center for Research in Security Prices (CRSP),
601 in the form of the VWD index has been used.⁶ This is a capitalization-weighted index of all
602 domestic stocks on major US exchanges, with data used dating back to 1926. For calibration
603 purposes, the index is adjusted for inflation prior to the calculation of returns.
- 604 • Risk-free rate: The risk-free rate is based on 3-month US T-bill rates for the period *1934:1-*
605 *2014:12*,⁷ augmented by National Bureau of Economic Research (NBER) short-term government
606 bond yields for *1926:1 - 1933:12*⁸ to incorporate the effect of the 1929 crash. More specifically,
607 a T-bill index is created, inflation-adjusted, then a sample average of the monthly returns is
608 calculated, and annualized to obtain the constant risk-free rate estimate r .

⁶More specifically, results presented here were calculated based on data from Historical Indexes, ©2015 Center for Research in Security Prices (CRSP), The University of Chicago Booth School of Business. Wharton Research Data Services was used in preparing this article. This service and the data available thereon constitute valuable intellectual property and trade secrets of WRDS and/or its third-party suppliers.

⁷See <http://research.stlouisfed.org/fred2/series/TB3MS>.

⁸See <http://www.nber.org/databases/macroeconomichistory/contents/chapter13.html>.

- Inflation: In order to adjust the time series for inflation, the annual average CPI-U index (inflation for urban consumers) from the US Bureau of Labor Statistics has been used.⁹

In order to avoid problems, such as multiple local maxima, ill-posedness, associated with the use of maximum likelihood estimation to calibrate the jump models, the thresholding technique of Cont and Mancini (2011); Mancini (2009) has been used, as applied in Dang and Forsyth (2016); Forsyth and Vetzal (2017), for the calibration. Specifically, if $\Delta\hat{X}_i$ denotes the i th inflation-adjusted, detrended log return in the historical risky asset index time series, we identify a jump in period i if

$$|\Delta\hat{X}_i| > \alpha\hat{\sigma}\sqrt{\Delta t}, \quad (5.1)$$

where $\hat{\sigma}$ is the estimate of the diffusive volatility, Δt is the time period over which the log return has been calculated, and α is the “threshold parameter” for identifying a jump. Distinguishing between “up” and “down” jumps for the Kou model is achieved using upward and downward jump indicators - see Forsyth and Vetzal (2017) for further details, including the simultaneous estimation of the diffusive volatility. We will use $\alpha = 3$ in what follows - in other words, we would only detect a jump in the historical time series if the (absolute, inflation-adjusted, and detrended) log return in that period exceeds 3 standard deviations of the “geometric Brownian motion change”, which is a very unlikely event. In the case of GBM, we use standard maximum likelihood techniques. The resulting calibrated parameters are provided in Table 5.1.

Table 5.1: Calibrated risky and risk-free asset process parameters ($\alpha = 3$ used in (5.1) for the Merton and Kou models).

Parameters	Models		
	GBM	Merton	Kou
μ (drift)	0.0816	0.0817	0.0874
σ (diffusive volatility)	0.1863	0.1453	0.1452
λ (jump intensity)	n/a	0.3483	0.3483
\tilde{m} (log jump multiplier mean)	n/a	-0.0700	n/a
$\tilde{\gamma}$ (log jump multiplier stdev)	n/a	0.1924	n/a
ν (probability of up-jump)	n/a	n/a	0.2903
ζ_1 (exponential parameter up-jump)	n/a	n/a	4.7941
ζ_2 (exponential parameter down-jump)	n/a	n/a	5.4349
r (Risk-free rate)	0.00623	0.00623	0.00623

5.2 Convergence analysis

In this subsection, we demonstrate that the numerical PDE solution converges to known analytical solutions available in special cases where such solutions are available, and rely on Monte Carlo simulation to verify results in the cases where analytical solutions are not available.

5.2.1 Analytical solutions

Analytical solutions for the time-consistent problem are available if the risky asset follows GBM (see Basak and Chabakauri (2010)) or any of the commonly-encountered jump models, including the Merton and Kou models (see Bjork and Murgoci (2010) and Zeng et al. (2013)), under the following

⁹CPI data from the U.S. Bureau of Labor Statistics. In particular, we use the annual average of the all urban consumers (CPI-U) index. See <http://www.bls.gov/cpi>.

634 assumptions: (i) continuous rebalancing of the portfolio, (ii) trading continues in the event of in-
635 solvency, (iii) no investment constraints or transaction costs, and (iv) same lending and borrowing
636 rate ($= r$). Under these assumptions, the efficient frontier solution is given by

$$\begin{aligned}
637 \quad E_{C_0^*}^{t=0} [W(T)] &= W(0) e^{rT} + \frac{1}{2\rho} \left[\frac{(\mu - r)^2}{\sigma^2 + \lambda\kappa_2} \right] T, \\
638 \quad Stdev_{C_0^*}^{t=0} [W(T)] &= \frac{1}{2\rho} \left(\frac{\mu - r}{\sqrt{\sigma^2 + \lambda\kappa_2}} \right) \sqrt{T}, \tag{5.2}
\end{aligned}$$

639 where we set $\lambda = 0$ to obtain the special solution in the case where the risky asset follows GBM.

640 Table 5.2 provides the timestep and grid information for testing convergence to the analytical
641 solution (5.2). While equal timesteps are used, the grids in the s - and b -directions are not uniform.

Table 5.2: Grid and timestep refinement levels for convergence analysis to the analytical solution (5.2)

Refinement level	Timesteps	s -grid nodes	b -grid nodes
0	30	70	147
1	60	139	293
2	120	277	585
3	240	553	1089

641 Table 5.3 illustrates the numerical convergence analysis for an initial wealth of $W(0) = 100$,
642 maturity $T = 10$ years, and scalarization parameter $\rho = 0.005$. For illustrative purposes, we assume
643 the risky asset follows the Merton model - qualitatively similar results are obtained if the Kou or GBM
644 models are assumed. The “Error” column shows the difference between the analytical solution and
645 the PDE solution, while the “Ratio” column shows the ratio of successive errors for each increase in
646 the refinement level. We observe first-order convergence of the numerical PDE efficient frontier values
647 to the analytical values obtained from (5.2) as the mesh is refined, which is expected.

Table 5.3: Convergence to analytical solution - Merton model

Refinement level	Expected value (Analytical solution: 274.5)			Standard deviation (Analytical solution: 129.7)		
	PDE solution	Error	Ratio	PDE solution	Error	Ratio
0	250.7	23.8	-	120.2	9.5	-
1	263.1	11.4	2.08	125.2	4.6	2.08
2	269.2	5.3	2.16	127.7	2.1	2.22
3	272.0	2.5	2.13	128.7	1.0	2.01

648

649 5.2.2 Monte Carlo validation

650 Consider now the following case where analytical solutions are *not* available: we assume discrete
651 periodic rebalancing of the portfolio at the end of each year, with liquidation in the event of insolvency,
652 and a maximum allowable leverage ratio of $q_{\max} = 1.5$. Additionally, we assume the risky asset follows
653 the Kou model, with initial wealth of $W(0) = 100$, maturity $T = 20$ years, and scalarization parameter
654 $\rho = 0.0014$. For the numerical PDE solution, using 7,280 equal timesteps, and 1,121 and 2,209 s -grid
655 and b -grid nodes, respectively, we obtain the following approximations to the expectation and standard
656 deviation:

$$657 \quad \left(E_{C_0^*}^{t=0} [W(T)], Stdev_{C_0^*}^{t=0} [W(T)] \right) = (544.58, 400.20). \tag{5.3}$$

658 At each timestep of our numerical PDE procedure, we output and store the computed optimal strategy
659 for each discrete state value. We then carry out Monte Carlo simulations for the portfolio (using the
660 specified parameters) from $t = 0$ to $t = T$, rebalancing the portfolio in accordance with the stored
661 PDE-computed optimal strategy at each discrete rebalancing time. If necessary, we use interpolation to
662 determine the optimal strategy for a given state value. We then compare the Monte Carlo computed
663 means and standard deviations of the terminal wealth with the corresponding values computed by
664 the numerical PDE method, given in (5.3). The results are shown in Table 5.4. Note that, for the
665 MC method, due to the possibility of insolvency, it is not possible to take finite timesteps between
rebalancing times without incurring timestepping errors.

Table 5.4: Convergence analysis to numerical PDE solution using Monte Carlo simulation - Kou model.

Nr of simulations	Nr of timesteps / year	Expectation (PDE solution: 544.58)		Standard deviation (PDE solution: 400.20)	
		Value	Relative error	Value	Relative error
4,000	728	537.03	-1.39%	388.69	-2.88%
16,000	1,456	540.28	-0.79%	391.48	-2.18%
64,000	2,912	540.92	-0.67%	396.80	-0.85%
256,000	5,824	542.60	-0.36%	398.38	-0.46%
1,024,000	11,648	544.33	-0.05%	399.08	-0.28%

666 We observe that, as the number of Monte Carlo simulations and timesteps increase, the Monte
667 Carlo computed means and standard deviations converge to the corresponding values computed by
668 the numerical PDE method, given in (5.3).
669

670 5.3 Time-consistent MV efficient frontiers

671 In this subsection, we study time-consistent MV efficient frontiers. All efficient frontier results in this
672 section are based on an initial wealth of $W(0) = 100$ and a maturity $T = 20$ years, along with annual
673 (discrete) rebalancing, and approximately daily interest payments (364 payments per year) on the
674 amount in the risk-free asset. To construct a point on the efficient frontier via the PDE scheme, we
675 use 7,280 equal timesteps, and 561 and 1,105 s -grid and b -grid nodes, respectively.

676 In order to consider the impact of investment constraints and other assumptions, including trans-
action costs, we construct five experiments as outlined in Table 5.5. We highlight the following:

Table 5.5: Details of experiments

Experiment	Lending/ borrowing rates		If insolvent	Leverage constraint	Transaction costs	
	r_ℓ	r_b			Fixed (c_1)	Prop. (c_2)
Experiment 1	0.00623	0.00623	Continue trading	None	0	0
Experiment 2	0.00623	0.00623	Liquidate	None	0	0
Experiment 3	0.00623	0.00623	Liquidate	$q_{\max} = 1.5$	0	0
Experiment 4	0.00400	0.06100	Liquidate	$q_{\max} = 1.5$	0	0
Experiment 5	0.00400	0.06100	Liquidate	$q_{\max} = 1.5$	0.001	0.005

677

- The interest rates for Experiments 4 and 5 were obtained by assuming that the approximate relationship between current interest rates paid on margin accounts in relation to current 3-month US T-bill rates¹⁰, also holds in relation to the historically observed 3-month US T-bill rates used to obtain the constant rate of 0.00623 (see Table 5.1).
- The transaction costs in the case of Experiment 5 are perhaps somewhat extreme. As in the case of Dang and Forsyth (2014), the costs were chosen to emphasize the effect of transaction costs in particular when compared to an Experiment 4 (which has the same borrowing/lending rates as Experiment 5, but with zero transaction costs).

5.3.1 Model choice

We consider the efficient frontiers obtained for the time-consistent MV problem using the numerical PDE scheme as outlined above, starting with the impact of model choice, namely GBM, Merton, or Kou dynamics, on the efficient frontiers. In Figure 5.1, we present the time-consistent MV efficient frontiers for Experiments 1 and 2, with the risky asset dynamics following GBM, Merton and Kou models. We observe that the Kou model results in a lower efficient frontier relative to the GBM and Merton models, whose efficient frontiers are basically indistinguishable.

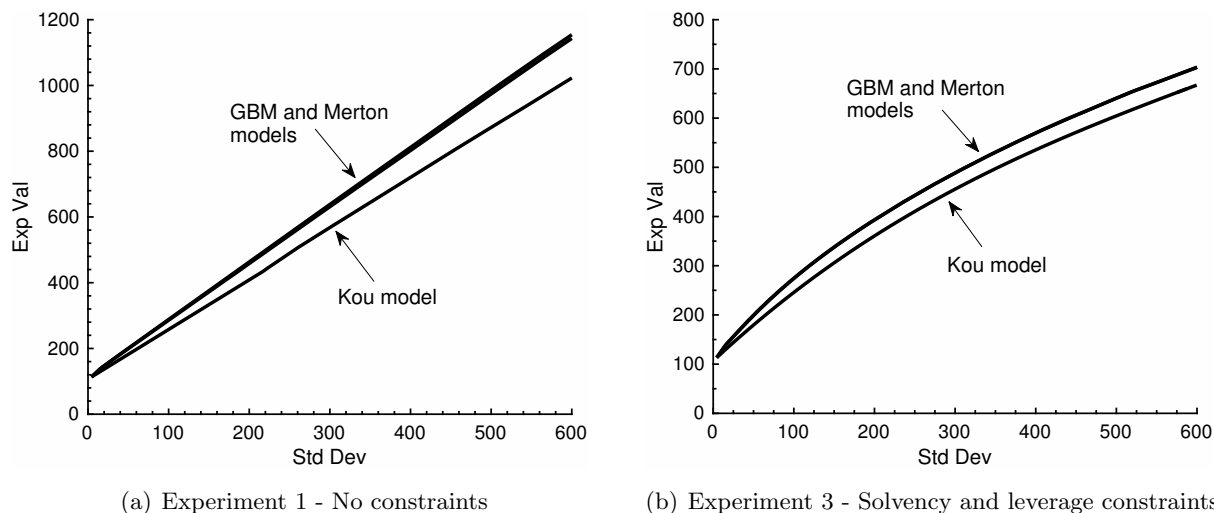


Figure 5.1: Time-consistent MV efficient frontiers - Effect of model choice (GBM, Merton, Kou)

Since these results are obtained using discrete (annual) rebalancing of the portfolio, no analytical solution exists, even in the case of the Experiment 1 frontiers seen in Figure 5.1(a). However, if we assume continuous rebalancing of the portfolio and no constraints, we can use the analytical solution in (5.2) to guide our intuition. Note that (5.2) can be re-arranged to give the expected value in terms of the standard deviation,

$$E_{C_0^*}^{t=0} [W(T)] = W(0) e^{rT} + \left(\frac{\mu - r}{\sqrt{\sigma^2 + \lambda \kappa_2}} \right) \sqrt{T} \cdot \left(Stdev_{C_0^*}^{t=0} [W(T)] \right). \quad (5.4)$$

¹⁰The interest paid/charged currently on margin accounts at major stockbrokers can be obtained with relative ease. For these experiments, the information was obtained as follows. On 15 March 2017, Merrill Edge (an online brokerage service of the Bank of America Merrill Lynch) charged roughly 5.75% on negative balances in margin accounts - the exact rate can depend on a number of factors. At that time, the short-term deposit rates of 0.03% paid by Bank of America was used as the interest rate paid on positive balances. These figures were then inflation-adjusted and scaled with the difference between current and historical real returns on T-bills, so that we assume in effect that the observed spread (difference between borrowing and lending rates) remained the same historically as they were in early 2017. This resulted in the rates of 6.10% and 0.40% shown in Table 5.5.

699 Fixing a standard deviation value on the efficient frontier, we observe that the effect of model
700 choice on the associated expected value on the efficient frontier is entirely due to the multiplier
701 $(\mu - r) / \sqrt{\sigma^2 + \lambda\kappa_2}$ in (5.4). With calibrated process parameters as given in Table 5.1, we have
702 combinations of parameters as given in Table 5.6. In particular, we conclude that the multiplier
703 $(\mu - r) / \sqrt{\sigma^2 + \lambda\kappa_2}$ is lower for the Kou model, due to the higher variance of the log-double exponential
704 distribution of the jump multipliers (resulting in a higher value of $\kappa_2 = \mathbb{E}[(\xi - 1)^2] = Var(\xi) + \kappa^2$)
705 compared to the that of the lognormal distribution in the case of the Merton model. We also note
706 that, as observed from Table 5.6, both the GBM and Merton models have almost the same value of
the multiplier $(\mu - r) / \sqrt{\sigma^2 + \lambda\kappa_2}$.

Table 5.6: Combinations of parameters ($\alpha = 3$ used in (5.1) for the Merton and Kou models)

Combinations of parameters	GBM	Merton	Kou
$\kappa = \mathbb{E}[(\xi - 1)]$	0.0000	-0.0502	-0.0338
$\kappa_2 = \mathbb{E}[(\xi - 1)^2]$	0.0000	0.0365	0.0844
$(\mu - r) / \sqrt{\sigma^2 + \lambda\kappa_2}$	0.4046	0.4103	0.3612

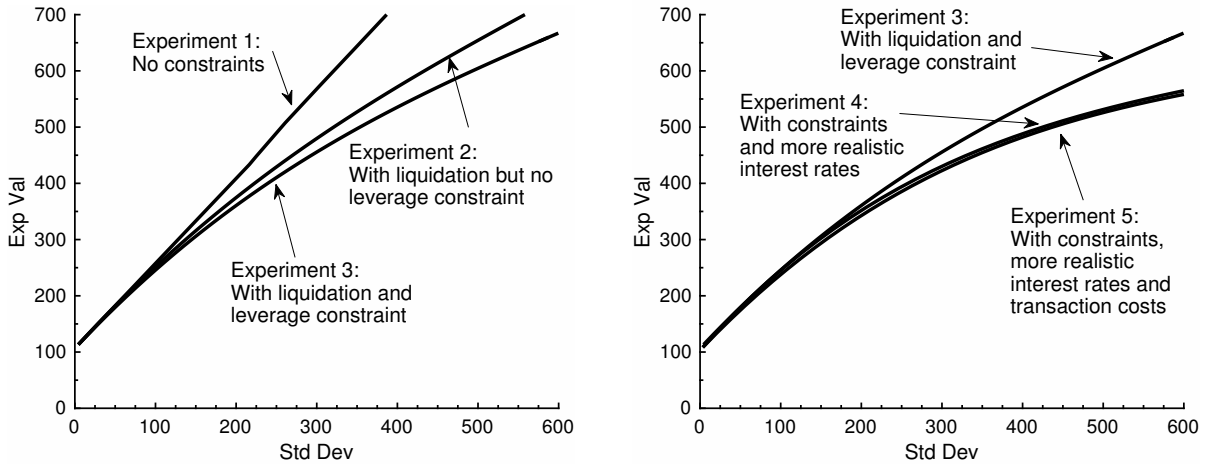
707
708 Returning to the results shown in Figure 5.1 where no analytical solutions are available, we conclude
709 the following. With the exception of parameters affecting the jump distribution, the other model
710 parameters (drift, diffusive volatility, jump intensity) of the Kou and Merton models in Table 5.1 are
711 very similar. Since the jump multipliers have a higher variance in the Kou model compared to the
712 Merton model (both calibrated to the same data), then for a given level of expected terminal wealth,
713 the Kou model results in a larger standard deviation of the terminal wealth. Consequently, the efficient
714 frontier is lower for the Kou model than for the Merton model. Furthermore, similar multiplier values
715 for the GBM and Merton models (observed above) imply that the relatively higher diffusive volatility
716 of the GBM model has a similar effect as the incorporation of jumps using the Merton model over this
717 long investment time horizon, resulting in similar efficient frontiers for the GBM and Merton models.

718 5.3.2 Investment constraints

719 The effect of investment constraints on the time-consistent MV efficient frontiers are shown in Figure
720 5.2 for the Kou model only, since the results for other models are qualitatively similar.

721 Figure 5.2(a) illustrates the significant impact of requiring liquidation in the event of insolvency
722 (Experiment 1 vs. Experiment 2). Furthermore, it is observed that, once liquidation in the event
723 of insolvency is a requirement, the impact of the leverage constraint is comparatively much smaller
724 (Experiment 2 vs. Experiment 3).

725 If we additionally incorporate more realistic interest rates, i.e. different lending and borrowing
726 rates, (Experiment 4), then Figure 5.2(b) shows a substantial reduction in the expected terminal
727 wealth that can be achieved, especially for high levels of risk. (Compare Experiments 3 and 4 on
728 Figure 5.2(b).) The reason for this is that, in order to achieve a high standard deviation of terminal
729 wealth, a comparatively large amount needs to be invested in the risky asset, which is achieved by
730 borrowing to invest. If the cost of borrowing is substantially increased (Experiment 4 vs. Experiment
731 3), the achievable expected terminal wealth reduces, reflecting the increased effective cost of executing
732 such a strategy. By comparison, the effect of additionally introducing transaction costs (Experiment
733 5) is relatively negligible.



(a) Effect of liquidation and leverage constraints

(b) Effect of interest rates and transaction costs

Figure 5.2: Time-consistent MV efficient frontiers - Kou model: Effect of investment constraints

5.4 Time-consistent MV vs. Pre-commitment MV strategies

In this section, we compare the time-consistent and the pre-commitment strategies, not only in terms of the resulting efficient frontiers, but also in terms of the optimal investment policies over time. We focus on the Kou model, since the other models yield qualitatively similar results. Process parameters are as in Table 5.1, investment parameters are as outlined at the beginning of Subsection 5.3, and details of the experiments are as in Table 5.5. The pre-commitment MV problem is formulated using impulse controls and solved according to the techniques outlined in Dang and Forsyth (2014). In order to provide a *fair* comparison with the standard time-consistent formulation, we do not optimally withdraw cash for the pre-commitment MV case (Cui et al., 2012; Dang and Forsyth, 2016). Allowing optimal cash withdrawals will move the efficient upward for the pre-commitment MV strategy.

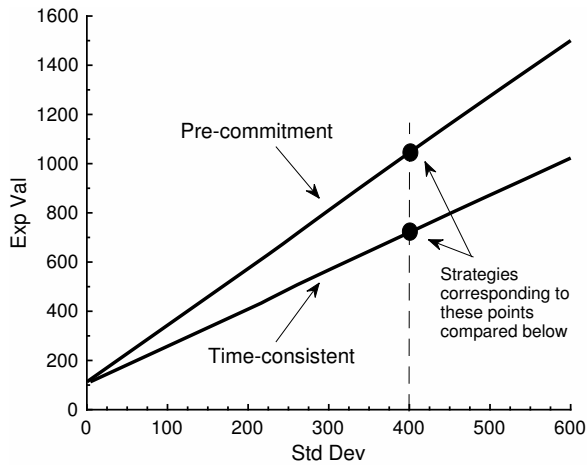
5.4.1 Combined investment constraints

Figure 5.3 compares the efficient frontiers associated with the pre-commitment and time-consistent problems in Experiments 1 and 3. As expected, the pre-commitment strategy is more MV efficient in the sense that the associated efficient frontier lies above that of the time-consistent strategy. This follows since the time-consistent problem carries the additional time-consistency constraint. However, under both the solvency and leverage constraints (Figure 5.3(b)), the difference between the two efficient frontiers is substantially reduced. A similar effect has also been observed in Wang and Forsyth (2011) for the case of continuous trading and no jumps in the risky asset process.

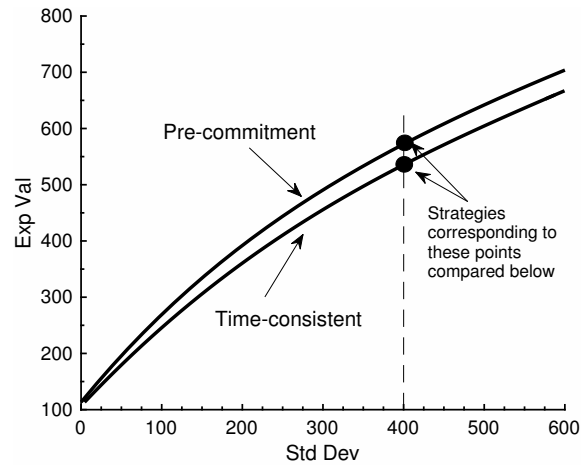
In Figures 5.3a and 5.3b, points on the efficient frontiers corresponding to a standard deviation of terminal wealth equal to 400 have been highlighted. The resulting MV-optimal strategies corresponding to these points will be investigated in more detail below (see Subsection 5.4.3).

5.4.2 Leverage constraint

Next, we focus on the impact of the leverage constraint. Figure 5.4 illustrates the effect of different maximum leverage constraint q_{\max} assumptions on the efficient frontiers associated with the pre-commitment and time-consistent MV problems. (In these tests, the solvency constraint is also imposed.) Since leverage may not be allowed for pension fund investments, we also consider the effect of setting $q_{\max} = 1$ (so that the fraction of total wealth invested in the risky asset may not exceed one) in Experiment 3.



(a) Experiment 1 - No constraints

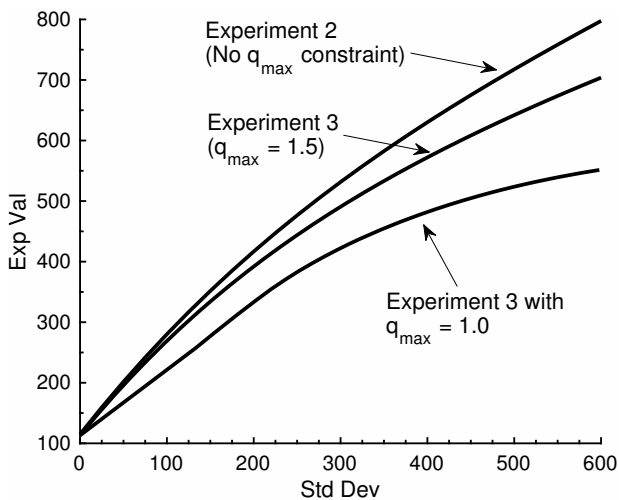


(b) Experiment 3 - Solvency and leverage constraints

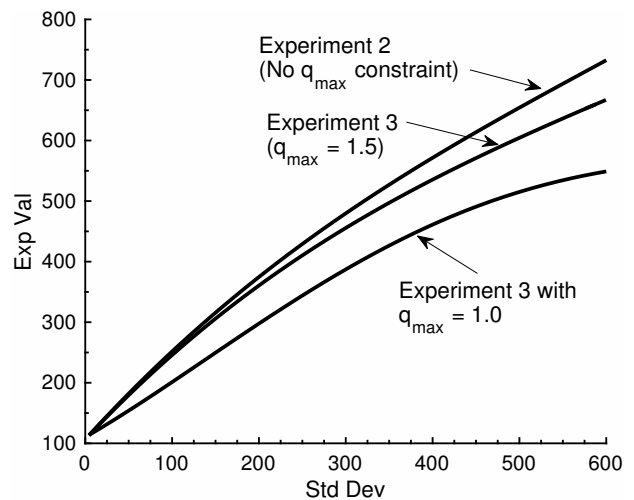
Figure 5.3: Pre-commitment MV vs. Time-consistent MV efficient frontiers - Kou model

762 It is observed that the effect on the efficient frontiers of not allowing leverage is quite dramatic.
 763 Interestingly, especially for high standard deviation of terminal wealth, the effect of setting $q_{\max} = 1$
 764 on the pre-commitment efficient frontier (Figure 5.4(a)) is comparatively larger than the effect on the
 765 time-consistent efficient frontier (Figure 5.4(b)).

766 The above observation is not entirely unexpected. As shown below (subsection 5.4.3), the pre-
 767 commitment MV optimal strategy generally favors much higher investment in the risky asset during
 768 the early years of the investment period, compared to the time-consistent MV optimal strategy. (See
 769 Figures 5.7 and 5.6 and the relevant discussion). Not allowing any leverage, therefore, has a larger
 770 relative impact on the pre-commitment MV efficient frontier.



(a) Pre-commitment strategy



(b) Time-consistent strategy

Figure 5.4: Pre-commitment MV vs. Time-consistent MV - Kou model: Effect of maximum leverage constraint q_{\max} .

771

772 5.4.3 Comparison of optimal controls

773 To gain further insight into the optimal control strategy of the time-consistency and pre-commitment
 774 approaches, we perform additional Monte Carlo simulations, using the same steps outlined in Subsec-
 775 tion 5.2.2, to Experiments 1 and 3 previously reported in Figure 5.3 (a)-(b).

776 Specifically, we first fix the standard deviation of the terminal wealth at a value of 400, as shown
 777 in Figure 5.3 (a)-(b). When solving the pre-commitment and time-consistent problems corresponding
 778 to these points on the efficient frontiers, at each timestep of our numerical PDE procedure, we output
 779 and store the computed optimal strategy for each discrete state value. We then carry out Monte Carlo
 780 simulations for the portfolio, using the specified parameters, from $t = 0$ to $t = T$, rebalancing the
 781 portfolio in accordance with the stored PDE-computed optimal strategy at each discrete rebalancing
 782 time. We compute, for each path and for each point in time, the fraction of wealth invested in the
 783 risky asset.

784 The results of this study are summarized in Figure 5.5 and Figure 5.6, where we show the median
 785 (50th percentile), as well as the 25th and 75th percentiles, of the distribution of the MV-optimal
 786 fraction of wealth invested in the risky asset over time.

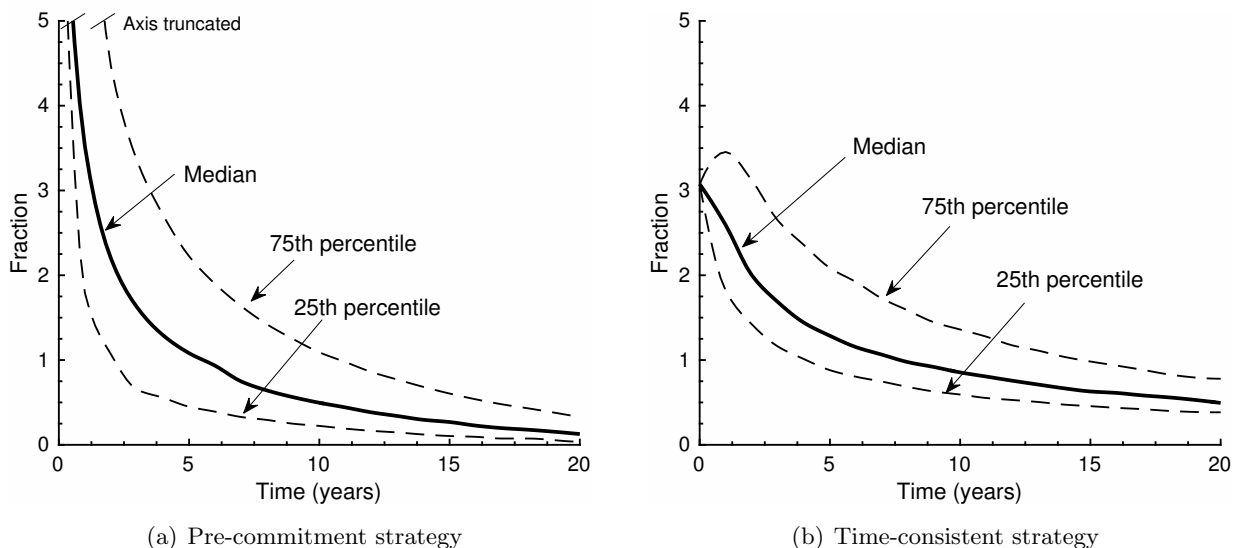


Figure 5.5: MV-optimal fraction of wealth in the risky asset: Kou model, Experiment 1, standard deviation of terminal wealth equal to 400.

787 Figure 5.5 compares the fraction of wealth in the risky asset for Experiment 1 (no investment
 788 constraints). In the case of the pre-commitment strategy (Figure 5.5(a)), the investment in the
 789 risky asset is initially much higher than in the case of the time-consistent strategy (Figure 5.5(b)).
 790 This changes as time progresses, with the fraction of wealth invested in the risky asset decreasing
 791 substantially for the pre-commitment strategy. While a decrease can also be observed for the time-
 792 consistent strategy, it is much more gradual. Furthermore, at about $t = 3$ (years) in this case, the
 793 median fraction of wealth in the risky asset for the time-consistent strategy exceeds that of the pre-
 794 commitment strategy.

795 The above observation can be explained by recalling from Vigna (2014) that the pre-commitment
 796 problem can also be viewed as a target-based optimization problem, where a quadratic loss function
 797 is minimized. This means that once the portfolio wealth is sufficiently large, so that the (implicitly)
 798 targeted terminal wealth becomes more achievable, the pre-committed investor will reduce the risk
 799 by reducing the investment in the risky asset. In contrast, the time-consistent investor has no invest-
 800 ment target, and instead, acts consistently with the mean-variance risk preferences throughout the
 801 investment time horizon (see for example Cong and Oosterlee (2016) for a relevant discussion).

802 If we impose liquidation in the event of insolvency, as well as a maximum leverage ratio of $q_{\max} =$
 803 1.5, i.e. Experiment 3, Figure 5.6 shows that the resulting MV-optimal fraction of wealth invested
 804 in the risky asset changes substantially compared to Figure 5.5. In particular, we observe that the
 805 fraction invested in the risky asset for the pre-commitment strategy (Figure 5.6(a)) is more strongly

806 affected by the maximum leverage constraint than the fraction for the time-consistent strategy (Figure
 807 5.6(b)). While this only considers only one point on the efficient frontier, where the standard deviation
 808 of terminal wealth is equal to 400, we have observed the higher sensitivity of the pre-commitment
 809 strategy to the maximum leverage constraint across the efficient frontier in Figure 5.4. This is due to
 810 the very large pre-commitment MV-optimal investment in the risky asset required during the early
 811 stages of the investment time period in order to achieve the implicit wealth target. On the other hand,
 812 it is interesting to observe that the pre-commitment strategy at the 25th percentile shows a very rapid
 813 de-risking compared to the time-consistent strategy.

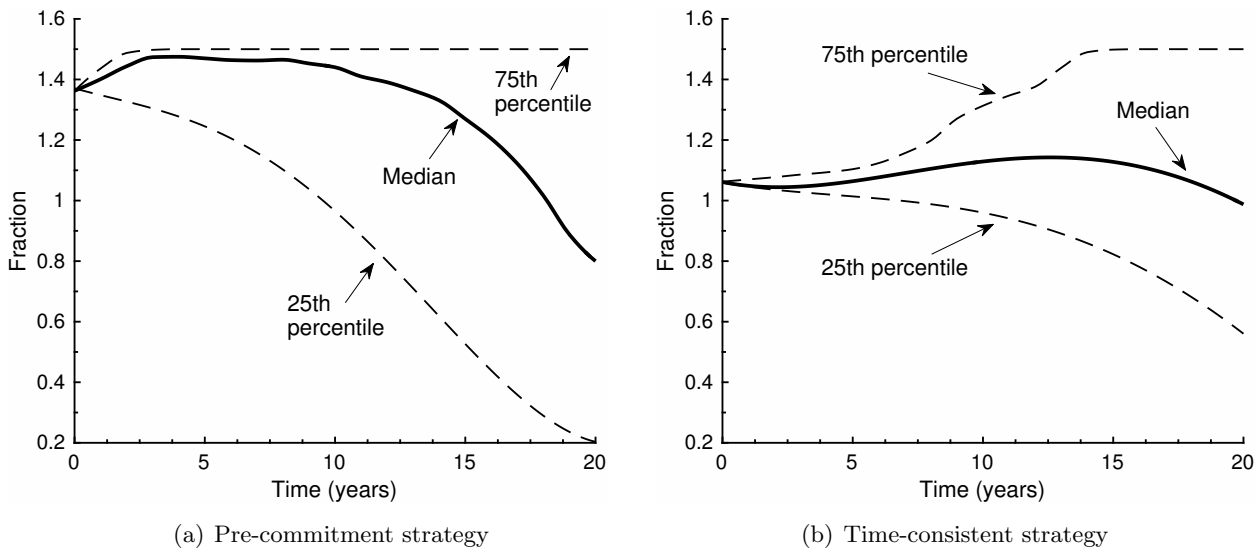


Figure 5.6: MV-optimal fraction of wealth in the risky asset: Kou model, Experiment 3, standard deviation of terminal wealth equal to 400.

814 To further investigate the differences between the pre-commitment and time-consistency optimal
 815 strategies, in Figure 5.7, we present the heatmaps of the MV-optimal control (as the fraction of
 816 wealth invested in the risky asset) as a function of time and wealth, which is used in the Monte Carlo
 simulation to generate the results in Figure 5.6.

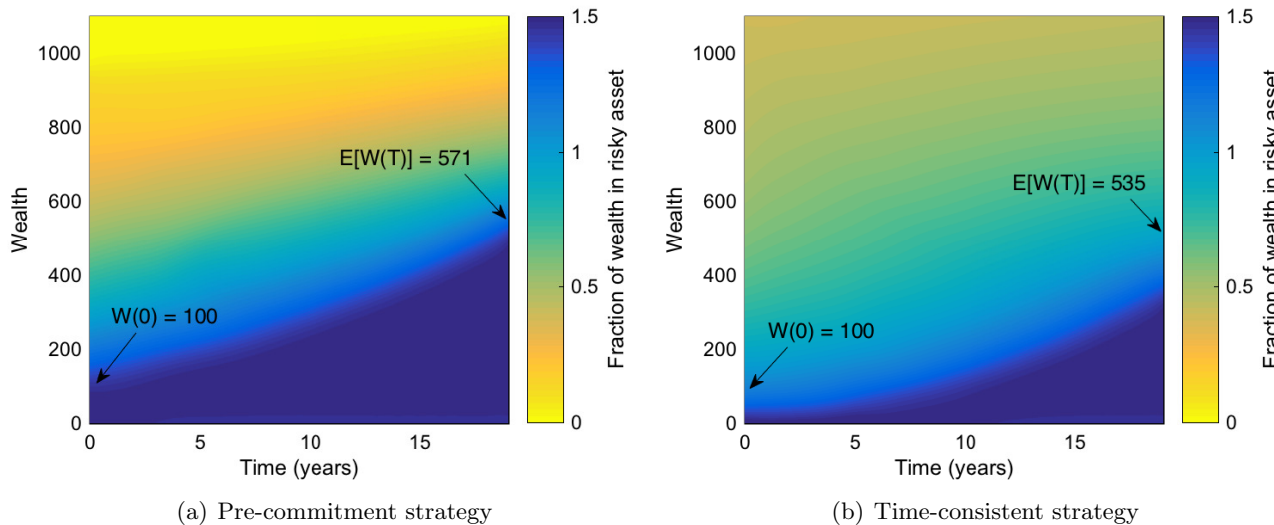


Figure 5.7: Optimal control as a fraction of wealth in risky asset: Kou model, Experiment 3, standard deviation of terminal wealth equal to 400.

817 We observe that, in the case of the pre-commitment optimal control (Figure 5.7(a)), for initial
818 wealth of $W(0) = 100$ the optimal control requires a very large investment (very close to the maximum
819 leverage of 1.5) in the risky asset. If returns are favourable - and therefore if wealth becomes sufficiently
820 large over time - the optimal control specifies a reduction in the investment in the risky asset, possibly
821 even to zero. If returns are unfavourable - so that wealth remains relatively small over time - the
822 optimal strategy requires a very large fraction of wealth (again very close, if not equal to, the maximum
823 leverage allowed) to remain invested in the risky asset. This is consistent with the interpretation of
824 the pre-commitment strategy as a target-based strategy. If it becomes likely that the target will be
825 achieved (past returns have been favourable), risk exposure is reduced; in contrast, if returns have
826 been unfavourable in the past, risk is increased in order to make the achievement of the target more
827 likely.

828 In contrast, in the case of the time-consistent optimal control (Figure 5.7(b)), there are a number of
829 qualitative similarities to the pre-commitment optimal control (Figure 5.7(a)), but also key differences.
830 Both of the strategies are contrarian, in the sense that all else being equal, investment in the risky
831 asset is increased if its returns in the past have been unfavourable. However, compared to the pre-
832 commitment optimal control, the time-consistent optimal control requires generally higher investment
833 in the risky asset if past returns have been favourable (resulting higher wealth), and lower investment
834 in the risky asset if past returns have been unfavourable (resulting in lower wealth). Even if the risky
835 asset performs extremely well, the time-consistent strategy never calls for zero exposure to the risky
836 asset. Figure 5.7 also shows why the pre-commitment strategy would be more heavily impacted if the
837 maximum leverage ratio is reduced; the time-consistent strategy calls for generally lower leverage, and
838 would therefore be less sensitive to the maximum leverage constraint.

839 5.5 Effect of a wealth-dependent scalarization parameter

840 Under the assumptions listed in Subsection 5.2.1 (in particular, under no investment constraints and
841 where trading continues in the event of bankruptcy), the time-consistent MV-optimal control leading
842 to the analytical efficient frontier solution in equation (5.2) does not depend on the investor's wealth
843 at any point in time - see Basak and Chabakauri (2010) and Zeng et al. (2013). In other words,
844 an investor following the resulting investment strategy is required to invest a particular *amount* in
845 the risky asset at each point in time, entirely independent of their available wealth, which is not an
846 economically reasonable conclusion. We emphasize that this is only true for the time-consistent MV
847 optimal control in the absence of any investment constraints.

848 To remedy this situation, Bjork et al. (2014) proposes the use of a state-dependent scalarization (or
849 risk aversion) parameter. Applied in our setting, we obtain a time-consistent MV problem otherwise
850 identical to equations (2.17) - (2.18), with the difference being that the risk aversion parameter at each
851 point in time is explicitly modelled by a deterministic function of the wealth $W(t)$, i.e. $\rho = \rho(W(t))$.
852 That is (2.17) now becomes

$$853 \sup_{C_t \in \mathcal{A}} \left(E_{C_t}^{x,t} [W(T)] - \rho(W(t)) \text{Var}_{C_t}^{x,t} [W(T)] \right)$$

854 In Bjork et al. (2014), it is argued that a natural choice for the function $\rho(W(t))$ is of the form

$$855 \rho(W(t)) = \frac{\theta}{W(t)}, \quad \theta > 0 \tag{5.5}$$

856 where for each θ , we obtain a point on the resulting efficient frontier. The use of a wealth-dependent
857 scalarization parameter has been popular in time-consistent MV literature within the non-constraint
858 setting, especially in insurance-related applications (see for example Zeng and Li (2011), Wei et al.
859 (2013), Li and Li (2013), as well as Liang and Song (2015)).

860 While some alternatives to (5.5) has also been suggested - see for example Bensoussan et al. (2014),
 861 we explore the effect of using the definition (5.5) in our setting, specifically because this simple case
 862 reveals how a seemingly reasonable definition of a wealth-dependent scalarization parameter, when
 863 used in combination with investment constraints and liquidation in the event of bankruptcy, can result
 864 in conclusions that are not economically reasonable.

865 Given Algorithm 3.1, implementing a wealth-dependent scalarization parameter such as (5.5) is
 866 straightforward, since we simply replace ρ in the algorithm with $\rho(W(s, b)) = \theta/W(s, b)$, where
 867 $W(s, b)$ is given by equation (2.8), without any further changes required. Varying $\theta > 0$ in this case
 868 traces out the efficient frontier.

869 We consider Experiment 3 in Table 5.5 (in other words we impose both liquidation in bankruptcy
 870 and a leverage constraint), since - as pointed out in Wang and Forsyth (2011) - allowing for negative
 871 wealth in equation (5.5) would lead to inappropriate risk aversion coefficients. In Figure 5.8, the
 872 efficient frontier obtained with a constant scalarization parameter ρ is compared with the efficient
 873 frontier obtained with wealth-dependent scalarization parameter of the form (5.5). We observe a
 874 similar result as in Wang and Forsyth (2011), where the case of continuous controls and no jumps was
 875 investigated: the resulting time-consistent MV efficient frontier with a wealth-dependent scalarization
 876 parameter is significantly lower than that obtained using a constant scalarization parameter. In
 877 other words, given an acceptable level of risk as measured by variance, a strategy based on the wealth-
 878 dependent scalarization parameter given by (5.5) would result in much lower expected terminal wealth,
 and is therefore less efficient from a MV-optimization perspective.

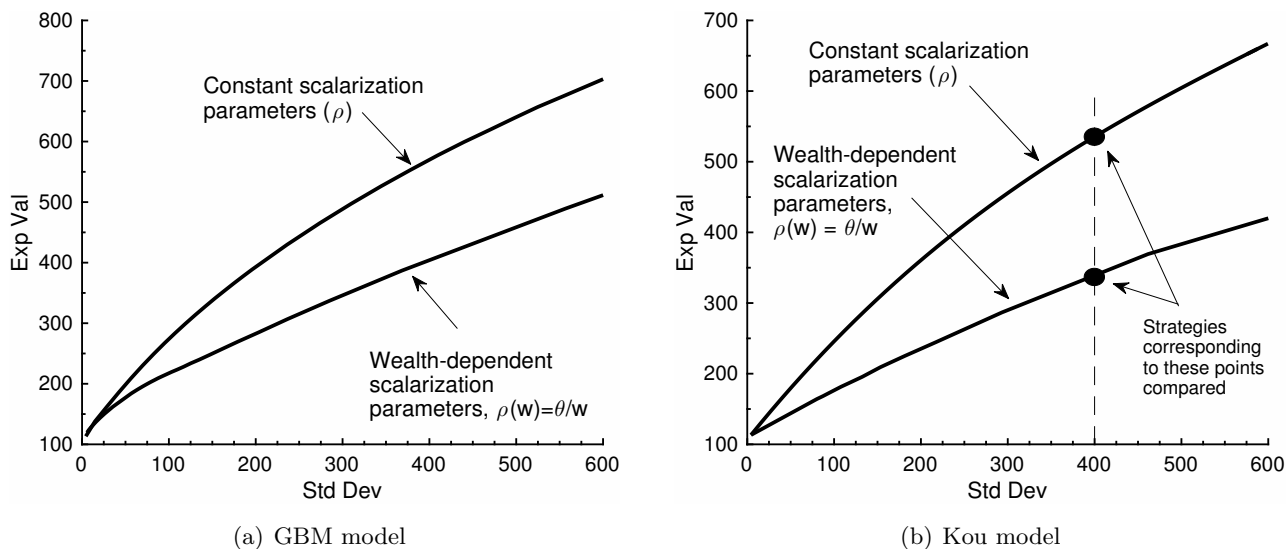
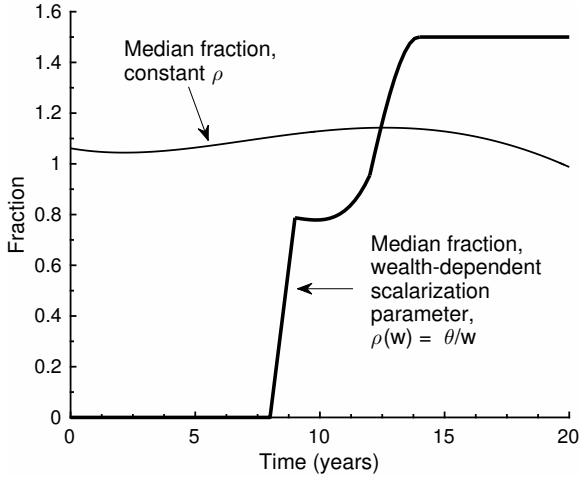


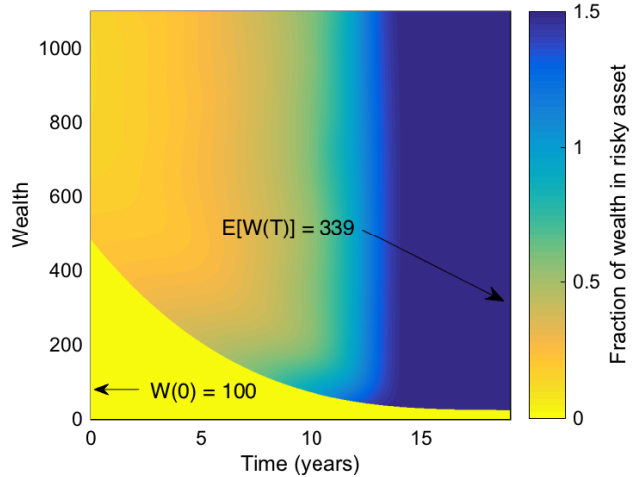
Figure 5.8: Time-consistent MV efficient frontiers - Experiment 3 (solvency and leverage constraints): Effect of using a constant scalarization parameter vs. using a wealth-dependent scalarization parameter of the form $\rho(w) = \theta/w$.

879 We now further compare the optimal trading strategies for the Kou model in both scenarios,
 880 namely a constant scalarization parameter and a wealth-dependent scalarization parameter of the
 881 form (5.5). In this case, we pick two points on the efficient frontiers corresponding to a standard
 882 deviation of terminal wealth equal to 400, as highlighted in Figure 5.8(b). In Figure 5.9, we now
 883 compare the resulting MV-optimal strategies corresponding to these points. Specifically, proceeding
 884 as in Subsection 5.4.3, using Monte Carlo simulations and rebalancing the portfolio in accordance
 885 with the stored PDE-computed optimal strategy at each discrete rebalancing time, we consider the
 886 resulting MV-optimal fraction of wealth invested in the risky asset over time.

888 Figure 5.9 (a) compares the median of the time-consistent MV-optimal fraction of wealth in the



(a) Median MV-optimal fraction of wealth in the risky asset



(b) Optimal control as fraction of wealth in risky asset, wealth-dependent scalarization parameter $\rho(w) = \theta/w$

Figure 5.9: Effect of using a using a wealth-dependent scalarization parameter of the form $\rho(w) = \theta/w$ on the median time-consistent MV-optimal fraction of wealth in the risky asset and on the resulting optimal controls. Kou model - Experiment 3 (solvency and leverage constraints), standard deviation of terminal wealth equal to 400.

889 risky asset in both scenarios.¹¹ Figure 5.9 (b) illustrates the heatmap of the time-consistent MV-
 890 optimal control (as the fraction of wealth invested in the risky asset) as a function of time and wealth
 891 in the case of a wealth-dependent scalarization parameter of the form (5.5). The heatmap for the
 892 time-consistent MV-optimal control in the case of a constant scalarization parameter (also for the
 893 Kou model, Experiment 3, and a standard deviation of terminal wealth equal to 400) is provided in
 894 Figure 5.7(b).

895 We make the following interesting observations. While the increase in exposure to the risky asset
 896 over time has been observed in the case of the wealth-dependent risk aversion parameter in the setting
 897 of no jumps, constraints or bankruptcy (see, for example, Bjork et al. (2014)), in the case of realistic
 898 investment constraints this is even more dramatic. Such observed dramatic impact can be explained
 899 as follows. The form of the wealth-dependent risk aversion in (5.5) implies that the risk aversion
 900 is inversely related to wealth. As such, it is possible (and indeed observed in Figure 5.9 (a)) that
 901 the investment in the risky asset can be zero until wealth has grown sufficiently and/or the time to
 902 maturity has decreased sufficiently, to make an investment in the risky asset MV-optimal. The level
 903 of risk aversion then steadily decreases, ensuring that the maximum exposure to the risky asset (only
 904 limited by the leverage constraint in this case) is reached as the investment maturity is approached.

905 While the economic merits of such a strategy depends on the particular application, it is unlikely
 906 to be economically reasonable in institution-related applications of MV optimization (such as in the
 907 case of pension funds or insurance). Specifically, relatively low investments in the risky asset during
 908 early years (due to high risk aversion resulting from relatively lower wealth levels) might result in
 909 lower terminal wealth - indeed, the expectation of terminal wealth is substantially lower with wealth-
 910 dependent scalarization parameter of the form (5.5) - which in turn might make it harder to fund
 911 liabilities, while the increase in risky asset exposure over time does not actually reduce the variance
 912 of terminal wealth (compared to the case of a constant ρ).

913 Therefore, in contrast to, for example Li and Li (2013), we conclude that a wealth-dependent scalar-
 914 ization parameter defined by (5.5) does not appear well-suited for obtaining realistic time-consistent

¹¹For the constant scalarization scenario, this corresponds to the median line in Figure 5.6(b).

915 MV optimal strategies in the presence of investment constraints, since the resulting terminal wealth
916 is less MV-efficient (as compared with the results obtained using a constant scalarization parameter),
917 while the steady increase in risk exposure over time might be undesirable in many applications of
918 time-consistent MV optimization.

919 **6 Conclusions**

920 In this paper, we develop a fully numerical PDE approach to solve the investment-only time-consistent
921 MV portfolio optimization problem when the underlying risky asset follows a jump-diffusion process.
922 The algorithm developed allows for the application of multiple simultaneous realistic investment con-
923 straints, including discrete rebalancing of the portfolio, the requirement of liquidation in the event
924 of insolvency, leverage constraints, different interest rates for borrowing and lending, and transaction
925 costs. The semi-Lagrangian timestepping scheme of Dang and Forsyth (2014) is extended to the sys-
926 tem of equations for the time-consistent problem, resulting in a set of only one-dimensional PIDEs to
927 be solved at each timestep. While no formal proof of convergence is given, numerical tests, including
928 a numerical convergence analysis where analytical solutions are available, as well as the validation
929 of results using Monte Carlo simulation, indicate that the algorithm provides reliable and accurate
930 results.

931 The economic implications of investment constraints on the efficient frontiers and on the resulting
932 optimal controls have been explored in detail. The numerical results illustrate that these realistic
933 considerations can have a substantial impact on the efficient frontiers and associated optimal controls,
934 resulting in economically plausible conclusions. In addition, the results from the time-consistent
935 problem are compared to those of the pre-commitment problem, leading to the conclusion that the
936 time-consistent problem is less sensitive to the maximum leverage constraint than the pre-commitment
937 problem. In addition, we explored the consequences of implementing a popular form of a wealth-
938 dependent risk aversion parameter (where risk aversion is inversely related to wealth), and find that
939 the resulting optimal investment strategy has both undesirable terminal wealth outcomes and an
940 undesirable evolution of risk characteristics over time. Not only does this finding pose questions about
941 the use of such wealth-dependent risk aversion parameters in existing time-consistent MV literature,
942 but it also highlights the importance of incorporating realistic constraints in investment models.

943 As a result of the popularity of the application of time-consistent MV optimization to investment-
944 reinsurance problems (see for example Alia et al. (2016); Li et al. (2015c); Liang and Song (2015)),
945 we leave the extension of the algorithm from the investment-only case to the investment-reinsurance
946 problem for our future work.

947 **References**

- 948 Alia, I., F. Chighoub, and A. Sohail (2016). A characterization of equilibrium strategies in continuous-
949 time mean-variance problems for insurers. *Insurance: Mathematics and Economics* (68), 212–223.
- 950 Basak, S. and G. Chabakauri (2010). Dynamic mean-variance asset allocation. *Review of Financial*
951 *Studies* 23, 2970–3016.
- 952 Bensoussan, A., K. C. Wong, S. C. P. Yam, and S. P. Yung (2014). Time-consistent portfolio selection
953 under short-selling prohibition: From discrete to continuous setting. *SIAM Journal on Financial*
954 *Mathematics* 5, 153–190.
- 955 Bjork, T., M. Khapko, and A. Murgoci (2016). A theory of Markovian time-inconsistent stochastic
956 control in continuous time. *Working paper* .

- 957 Bjork, T. and A. Murgoci (2010). A general theory of Markovian time inconsistent stochastic control
958 problems. *Working paper* Available at <http://ssrn.com/abstract=1694759>.
- 959 Bjork, T. and A. Murgoci (2014). A theory of Markovian time-inconsistent stochastic control in
960 discrete time. *Finance and Stochastics* (18), 545–592.
- 961 Bjork, T., A. Murgoci, and X. Zhou (2014). Mean-variance portfolio optimization with state-dependent
962 risk aversion. *Mathematical Finance* (1), 1–24.
- 963 Cong, F. and C. Oosterlee (2016). On pre-commitment aspects of a time-consistent strategy for a
964 mean-variance investor. *Journal of Economic Dynamics and Control* 70, 178–193.
- 965 Cont, R. and C. Mancini (2011). Nonparametric tests for pathwise properties of semi-martingales.
966 *Bernoulli* (17), 781–813.
- 967 Cont, R. and P. Tankov (2004). *Financial modelling with jump processes*. Chapman and Hall / CRC
968 Press.
- 969 Crandall, M., H. Ishii, and P. Lions (1992). User’s guide to viscosity solutions of second order partial
970 differential equations. *Bulletin of the American Mathematical Society* 27(1), 1–67.
- 971 Cui, X., D. Li, S. Wang, and S. Zhu (2012). Better than dynamic mean-variance: Time inconsistency
972 and free cash flow stream. *Mathematical Finance* 22(2), 346–378.
- 973 Cui, X., L. Xu, and Y. Zeng (2015). Continuous time mean-variance portfolio optimization with
974 piecewise state-dependent risk aversion. *Optimization Letters (Springer)* pp. 1–11.
- 975 Dang, D. and P. Forsyth (2014). Continuous time mean-variance optimal portfolio allocation under
976 jump diffusion: A numerical impulse control approach. *Numerical Methods for Partial Differential*
977 *Equations* 30, 664–698.
- 978 Dang, D. and P. Forsyth (2016). Better than pre-commitment mean-variance portfolio allocation
979 strategies: A semi-self-financing Hamilton–Jacobi–Bellman equation approach. *European Journal*
980 *of Operational Research* (250), 827–841.
- 981 Dang, D., P. Forsyth, and Y. Li (2016). Convergence of the embedded mean-variance optimal points
982 with discrete sampling. *Numerische Mathematik* (132), 271–302.
- 983 d’Halluin, Y., P. Forsyth, and K. Vetzal (2005). Robust numerical methods for contingent claims
984 under jump diffusion processes. *IMA Journal of Numerical Analysis* (25), 87–112.
- 985 Forsyth, P. and K. Vetzal (2017). Dynamic mean variance asset allocation: Tests for robustness.
986 *International Journal of Financial Engineering* 4:2. 1750021 (electronic).
- 987 Hu, Y., H. Jin, and X. Zhou (2012). Time-inconsistent stochastic linear-quadratic control. *SIAM*
988 *Journal on Control and Optimization* 50(3), 1548–1572.
- 989 Kou, S. (2002). A jump-diffusion model for option pricing. *Management Science* 48(8), 1086–1101.
- 990 Li, D. and W.-L. Ng (2000). Optimal dynamic portfolio selection: multi period mean variance formu-
991 lation. *Mathematical Finance* 10, 387–406.
- 992 Li, D., X. Rong, and H. Zhao (2015a). Time-consistent reinsurance–investment strategy for a mean-
993 variance insurer under stochastic interest rate model and inflation risk. *Insurance: Mathematics*
994 *and Economics* 64, 28–44.

- 995 Li, D., X. Rong, and H. Zhao (2015b). Time-consistent reinsurance–investment strategy for an insurer
996 and a reinsurer with mean–variance criterion under the cev model. *Journal of Computational and*
997 *Applied Mathematics* 283, 142–162.
- 998 Li, Y. and Z. Li (2013). Optimal time-consistent investment and reinsurance strategies for mean–
999 variance insurers with state dependent risk aversion. *Insurance: Mathematics and Economics* 53,
1000 86–97.
- 1001 Li, Y., H. Qiao, S. Wang, and L. Zhang (2015c). Time-consistent investment strategy under partial
1002 information. *Insurance: Mathematics and Economics* 65, 187–197.
- 1003 Li, Z., Y. Zeng, and Y. Lai (2012). Optimal time-consistent investment and reinsurance strategies for
1004 insurers under Heston’s SV model. *Insurance: Mathematics and Economics* 51, 191–203.
- 1005 Liang, Z. and M. Song (2015). Time-consistent reinsurance and investment strategies for mean–
1006 variance insurer under partial information. *Insurance: Mathematics and Economics* 65, 66–76.
- 1007 Lioui, A. (2013). Time consistent vs. time inconsistent dynamic asset allocation: Some utility cost
1008 calculations for mean variance preferences. *Journal of Economic Dynamics and Control* (37), 1066–
1009 1096.
- 1010 Ma, K. and P. Forsyth (2016). Numerical solution of the Hamilton-Jacobi-Bellman formulation for
1011 continuous time mean variance asset allocation under stochastic volatility. *Journal of Computational*
1012 *Finance* 20:1, 1–37.
- 1013 Mancini, C. (2009). Non-parametric threshold estimation models with stochastic diffusion coefficient
1014 and jumps. *Scandinavian Journal of Statistics* (36), 270–296.
- 1015 Markowitz, H. (1952). Portfolio selection. *The Journal of Finance* 7(1), 77–91.
- 1016 Merton, R. (1976). Option pricing when underlying stock returns are discontinuous. *Journal of*
1017 *Financial Economics* 3, 125–144.
- 1018 Oksendal, B. and A. Sulem (2005). *Applied Stochastic Control of Jump Diffusions*. Springer.
- 1019 Pedersen, J. and G. Peskir (2017). Optimal mean-variance portfolio selection. *Mathematics and*
1020 *Financial Economics* (11), 137–160.
- 1021 Ramezani, C. and Y. Zeng (2007). Maximum likelihood estimation of the double exponential jump-
1022 diffusion process. *Annals of Finance* 3(4), 487–507.
- 1023 Sun, J., Z. Li, and Y. Zeng (2016). Precommitment and equilibrium investment strategies for defined
1024 contribution pension plans under a jump–diffusion model. *Insurance: Mathematics and Economics*
1025 (67), 158–172.
- 1026 Vigna, E. (2014). On efficiency of mean-variance based portfolio selection in defined contribution
1027 pension schemes. *Quantitative Finance* 14(2), 237–258.
- 1028 Vigna, E. (2016). On time consistency for mean-variance portfolio selection. *Working paper, Collegio*
1029 *Carlo Alberto* (476).
- 1030 Vigna, E. (2017). Tail optimality and preferences consistency for intertemporal optimization problems.
1031 *Working paper, Collegio Carlo Alberto* (502).
- 1032 Wang, J. and P. Forsyth (2008). Maximal use of central differencing for Hamilton–Jacobi–Bellman
1033 PDEs in finance. *SIAM Journal on Numerical Analysis* (46), 1580–1601.

- 1034 Wang, J. and P. Forsyth (2010). Numerical solution of the Hamilton-Jacobi-Bellman formulation for
1035 continuous time mean variance asset allocation. *Journal of Economic Dynamics and Control* 34,
1036 207–230.
- 1037 Wang, J. and P. Forsyth (2011). Continuous time mean variance asset allocation: A time-consistent
1038 strategy. *European Journal of Operational Research* (209), 184–201.
- 1039 Wei, J. and T. Wang (2017). Time-consistent mean-variance asset-liability management with random
1040 coefficients. *Insurance: Mathematics and Economics* (77), 84–96.
- 1041 Wei, J., K. Wong, S. Yam, and S. Yung (2013). Markowitz’s mean-variance asset-liability management
1042 with regime switching: A time-consistent approach. *Insurance: Mathematics and Economics* 53,
1043 281–291.
- 1044 Yu, P. (1971). Cone convexity, cone extreme points, and nondominated solutions in decision problem
1045 with multiobjectives. *Journal of Optimization Theory and Applications* (7), 11–28.
- 1046 Zeng, Y. and Z. Li (2011). Optimal time-consistent investment and reinsurance policies for mean-
1047 variance insurers. *Insurance: Mathematics and Economics* 49(1), 145–154.
- 1048 Zeng, Y., Z. Li, and Y. Lai (2013). Time-consistent investment and reinsurance strategies for mean-
1049 variance insurers with jumps. *Insurance: Mathematics and Economics* 52, 498–507.
- 1050 Zhang, C. and Z. Liang (2017). Portfolio optimization for jump-diffusion risky assets with common
1051 shock dependence and state dependent risk aversion. *Optimal control applications and methods* (38),
1052 229–246.
- 1053 Zhou, X. and D. Li (2000). Continuous time mean variance portfolio selection: a stochastic LQ
1054 framework. *Applied Mathematics and Optimization* 42, 19–33.
- 1055 Zhou, Z., H. Xiao, J. Yin, X. Zeng, and L. Lin (2016). Pre-commitment vs. time-consistent strate-
1056 gies for the generalized multi-period portfolio optimization with stochastic cash flows. *Insurance:
1057 Mathematics and Economics* (68), 187–202.